NATIONAL AERONAUTICS AND SPACE ADMINISTRATION

Technical Report 32-1320

Capsule System Advanced Development Sterilization Program

A. R. Hoffman
J. T. Wang
M. R. Christensen

JET PROPULSION LABORATORY
CALIFORNIA INSTITUTE OF TECHNOLOGY
PASADENA, CALIFORNIA

October 15, 1969

NATIONAL AERONAUTICS AND SPACE ADMINISTRATION

Technical Report 32-1320

Capsule System Advanced Development Sterilization Program

A. R. Hoffman
J. T. Wang
M. R. Christensen

JET PROPULSION LABORATORY
CALIFORNIA INSTITUTE OF TECHNOLOGY
PASADENA, CALIFORNIA

October 15, 1969

Prepared Under Contract No. NAS 7-100
National Aeronautics and Space Administration

Preface

The work described in this report was performed by the Project Engineering Division of the Jet Propulsion Laboratory.

Contents

Tables

Contents (contd)

Tables (contd)

Figures

Contents (contd)

Figures (contd)

Abstract

A primary objective of the Capsule System Advanced Development (CSAD) Program was to gain experience in critical new technologies, one of which was capsule sterilization. The sterilization objective was to develop and apply terminal sterilization requirements and operations in a manner so that they might be implemented for a possible early Mars mission. The sterilization program included constructing thermal analytical models, performing microbiological assay during the assembly of the capsule, calculating process times, determining process requirements and procedures, subjecting the lander to an engineering sterilization environment, and subjecting the capsule to a terminal sterilization cycle.

The CSAD sterilization process is shown to be representative of a conservative process that might be used to terminally sterilize a flight capsule.

Capsule System Advanced Development Sterilization Program

I. Introduction

The design and development of a Mars planetary entry and landing system was initiated at the Laboratory in January 1967. This program was designated Capsule System Advanced Development (CSAD). The mission and preliminary design given in the technical study for Mars 1971* was chosen as the starting point for the capsule system design. To provide a realistic framework for the program, the *Mariner* Mars 1969 spacecraft was assumed to be the bus portion of the planetary vehicle and the Mars 1971 launching period was used as the mission opportunity.

To implement the effort, individual subsystem development tasks in the existing advanced development programs were reoriented toward the CSAD design and were paced to a project schedule in an effort to make a rapid advancement in the required capabilities and technologies.

The objectives of the CSAD Program were:

(1) To provide a means for gaining experience in several critical and new technologies related to planetary capsule missions.

(2) To develop an understanding of the subsystems so that realistic performance estimates can be made.

(3) To obtain an improved understanding of planetary entry capsule system design and integration problems.

The approach was to design and fabricate a lander system. After performing functional tests, the lander was subjected to a heat sterilization cycle and an impact test.

*Casani, E. K., *Mars 71 Technical Study*, Engineering Planning Document 427. Jet Propulsion Laboratory, Pasadena, Calif., Aug. 15, 1966.

For the purposes of this report, this portion of the program is designated as phase 1. In phase 2, an entry system was designed, fabricated, and combined with the lander system to form the capsule system feasibility model. After functional testing, the feasibility model was subjected to a terminal sterilization environment followed by functional tests and inspection to evaluate the effects of sterilization on the equipment. The lander was then subjected to an impact test on a flat, unyielding surface.

II. Capsule Description

The details of the program, the mission profile, and the description of the hardware have been reported elsewhere.* However, for ease of understanding, an outline of the mission profile and a brief hardware description are included below.

When launched, the planetary vehicle (i.e., capsule and spacecraft bus) are placed on a trajectory that permits the spacecraft to fly by the planet at a predetermined distance. Nominally, ten days before planetary encounter, the capsule is released from the spacecraft bus. At this point, the sterilization canister is opened with the fore portion of the canister ejected and the aft portion remaining with the spacecraft bus. Following this sequence and after spin stabilization, the capsule is deflected away from the bus and placed on an impact trajectory with the planet. The entry profile is given in Fig. 1. The capsule begins transmitting engineering and science data as it enters the atmosphere. When the capsule speed decreases to transonic, a small lander is extracted and it descends to the planet surface on a 20-ft diameter parachute. After landing and releasing the parachute, the lander transmits back to earth the engineering, wind, pressure, temperature, water vapor, and atmospheric compositional analysis data.

*Casani, E. K., and Gerpheide, J. H., *Capsule System Advanced Development Program Report*, Document 760-29. Jet Propulsion Laboratory, Pasadena, Calif., July 15, 1968.

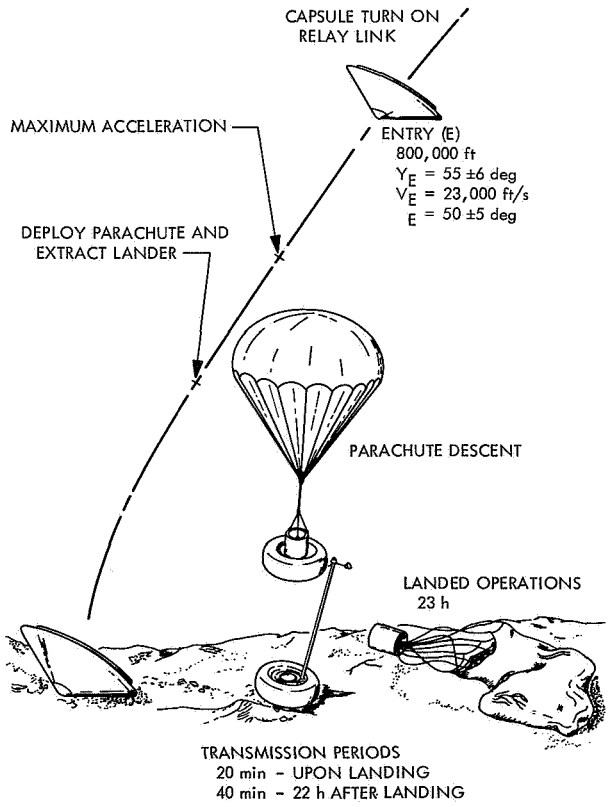

Fig. 1. Entry profile

The capsule mounted in its sterilization canister is depicted in Fig. 2. The capsule weight including the sterilization canister is 350 lb. The feasibility model hardware in the separation configuration is shown in Fig. 3 (the aeroshell is 6.5 ft in diameter). The lander modules and chassis with the impact limiter are shown in Fig. 4. The lander weighs approximately 50 lb and is 22 in. in diameter. The sterilization canister, including the biological filters for capsule pressure equalization, is shown in Fig. 5.

III. Assembly and Test

In phase 1 of the CSAD Program, a lander system was designed, fabricated, assembled, and tested as shown in Fig. 6. The subsystem hardware was delivered to the quality assurance bonded stores area of the Spacecraft Assembly Facility. After release from bonded stores, the hardware was assembled in the high bay area. After functional testing, the lander system was sterilized in a heating chamber at the Environmental Test Facility. An impact test was then performed at the Goldstone test site.

In phase 2, the feasibility model was assembled and tested as shown in Fig. 7. The delivery of the hardware and the assembly of the feasibility model occurred in the same area as phase 1. The sterilization test was performed in the terminal sterilization chamber.

Three sterilization tests were performed. These included: first, a dummy run using only the sterilization canister; second, a separate sterilization of the lander;

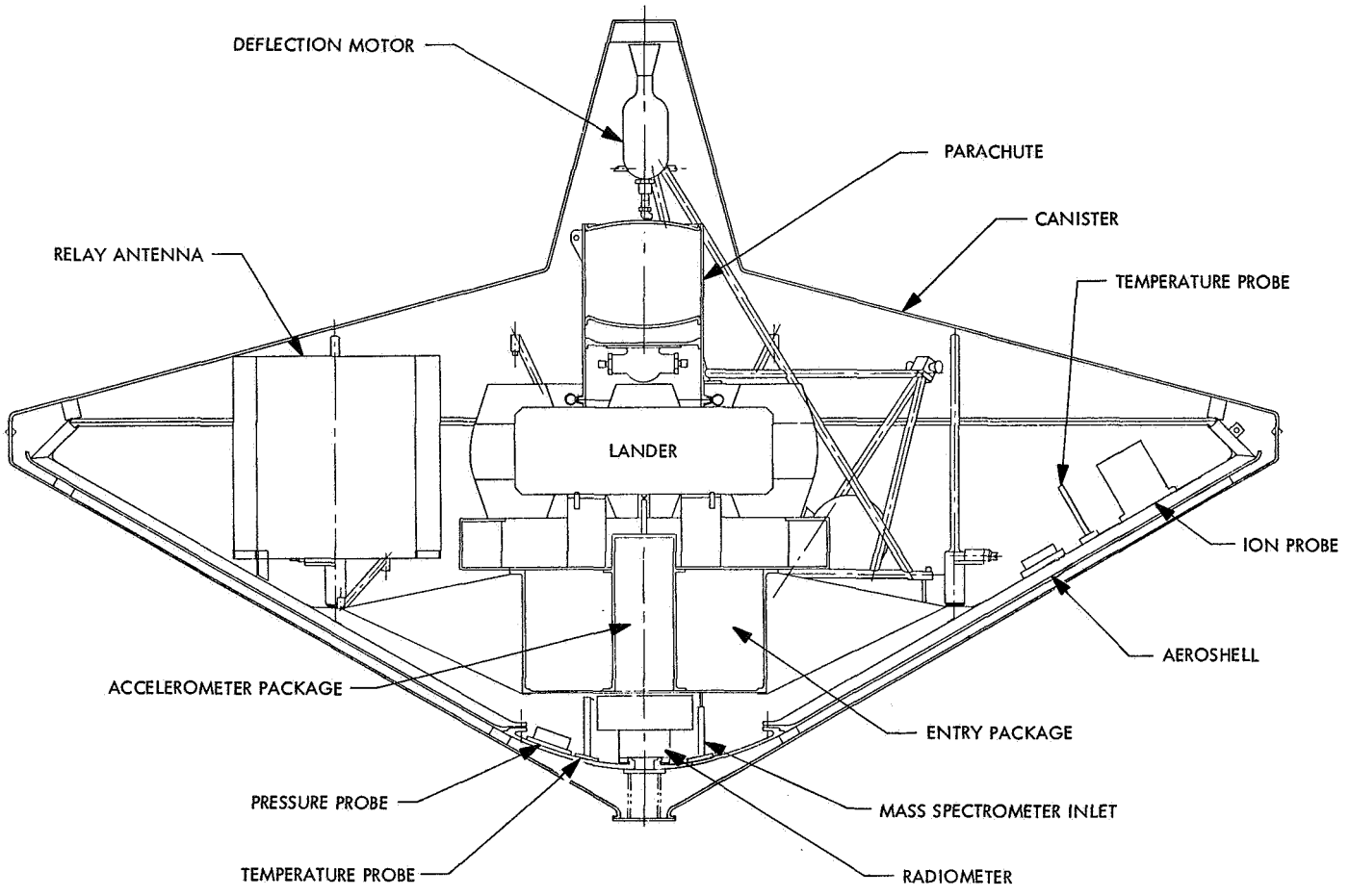

Fig. 2. Capsule cross section

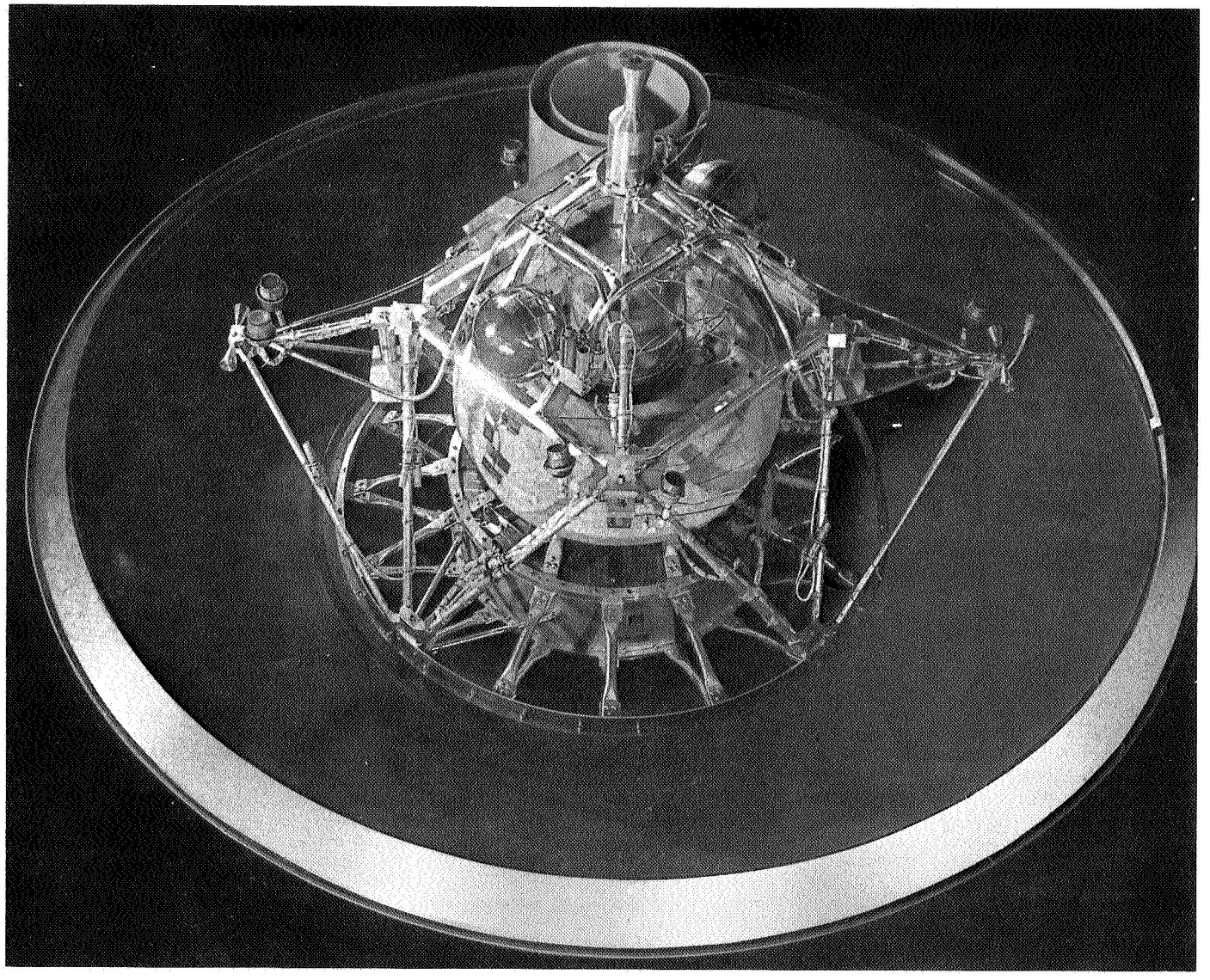

Fig. 3. Feasibility model, separation configuration

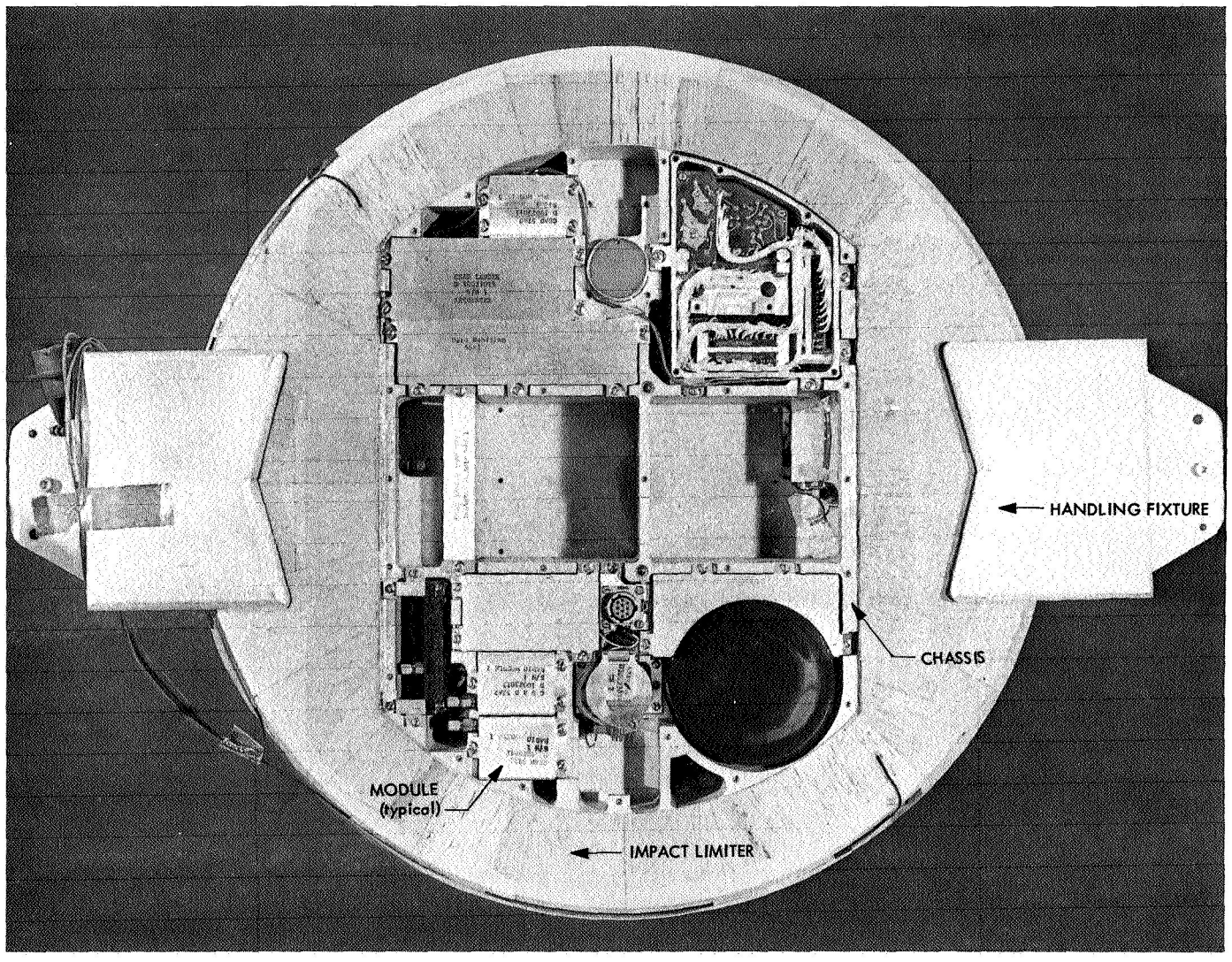

Fig. 4. Lander modules and chassis with impact limiter

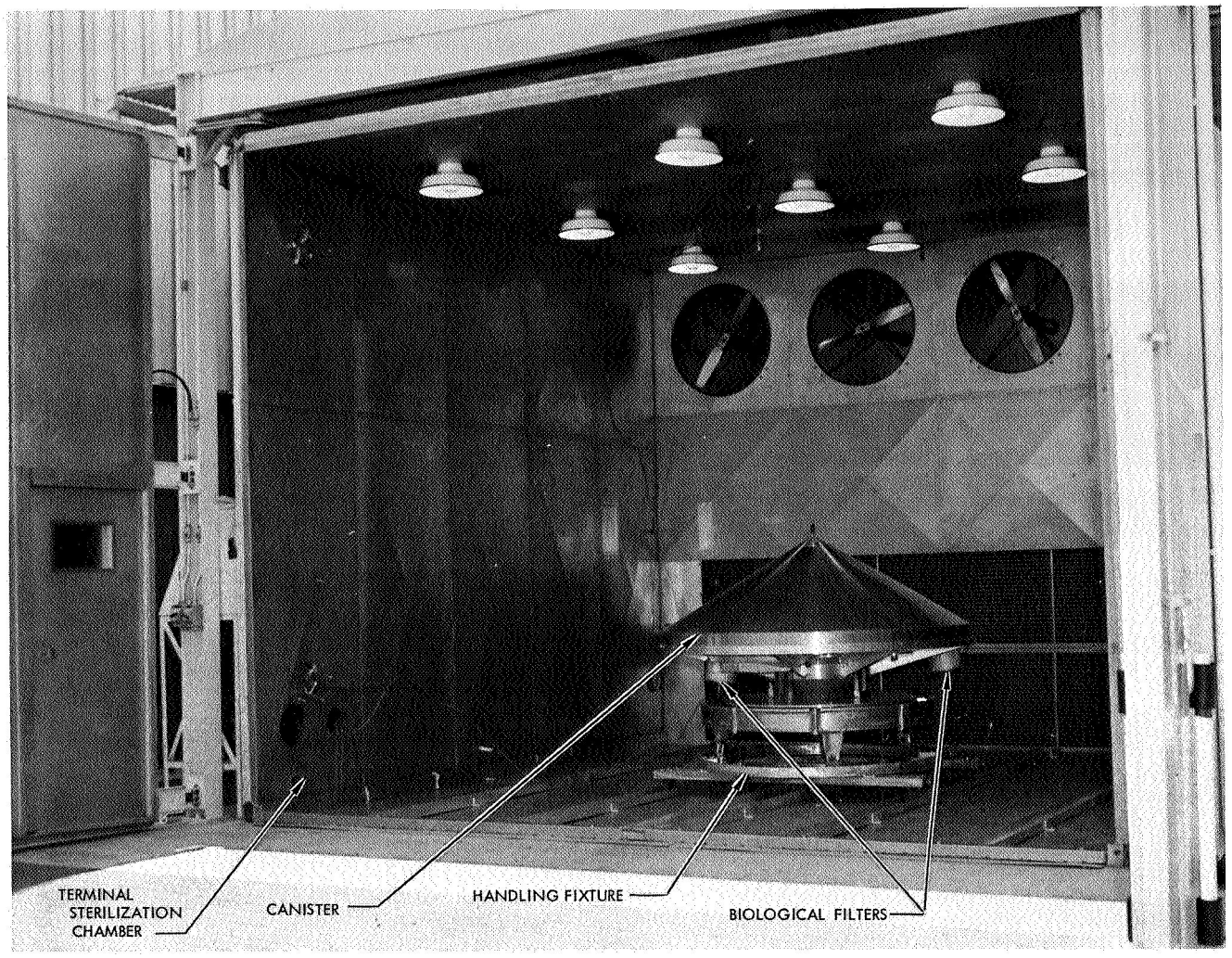

Fig. 5. CSAD feasibility model in the terminal sterilization chamber

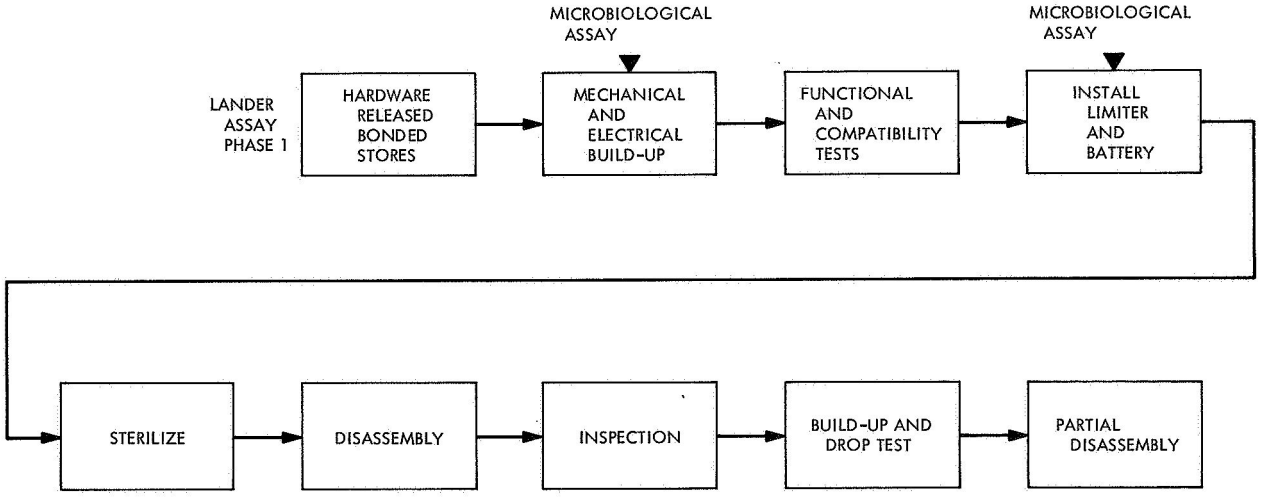

Fig. 6. Phase 1 flow of lander assembly sequence

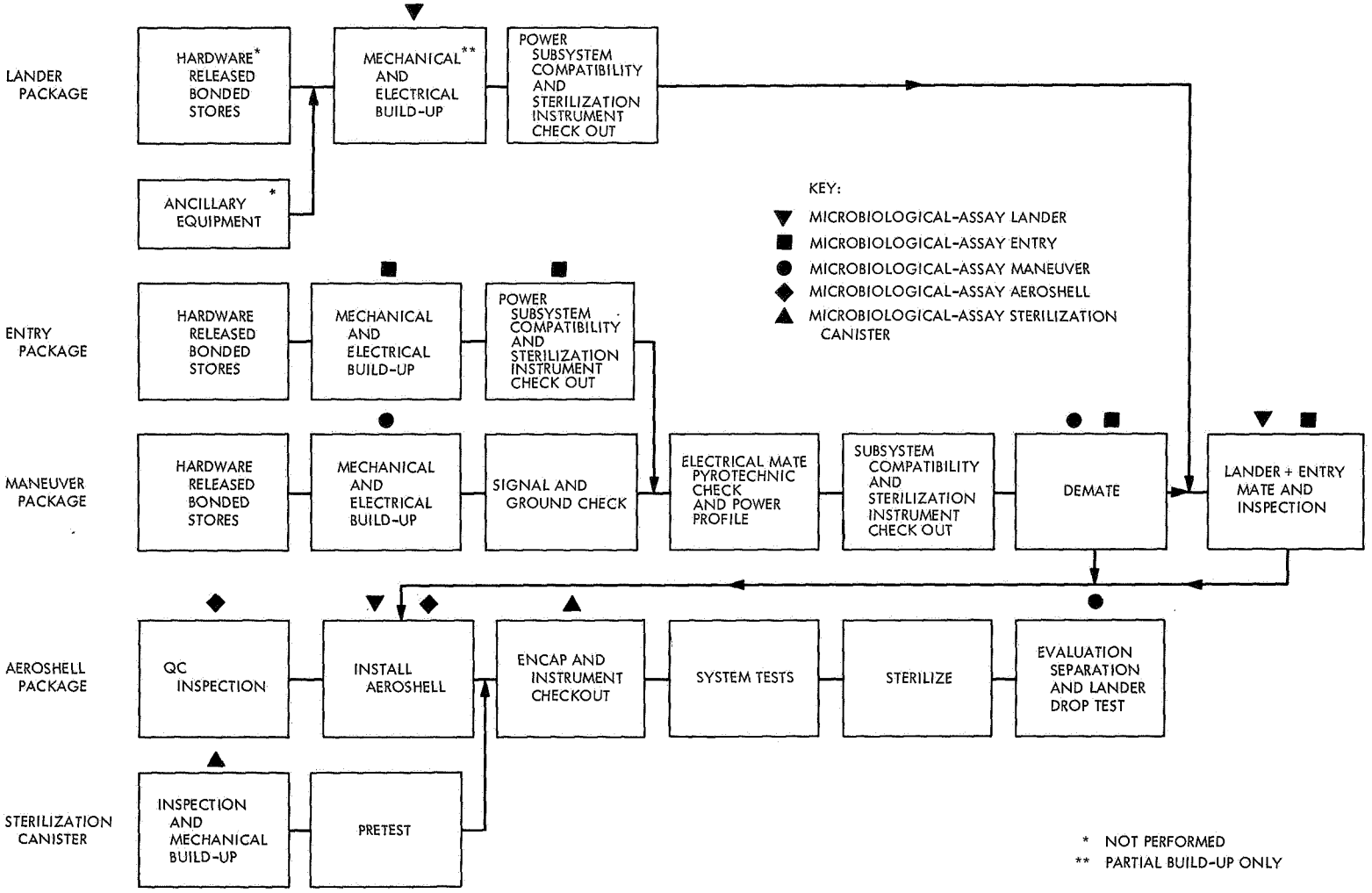

Fig. 7. Phase 2 flow of lander assembly sequence

and third, the CSAD feasibility model sterilization. The test objectives, configurations, requirements, instrumentation, and facilities are given in Table 1. Figures 5, 8, and 9 and Table 2 supplement Table 1. Test results will be discussed in Section VI.

The capsule sterilization tests consisted of four basic steps:

(1) Evacuate capsule and backfill with an inert gas (e.g., nitrogen) to minimize the possibility of oxidation of materials (capsule preconditioning).

(2) Install capsule in sterilization chamber.

(3) Purge chamber with inert gas.

(4) Perform sterilization process.

IV. Sterilization Process Determination

To determine sterilization parameters for a capsule, the following inputs are required (Ref. 1):

(1) Temperature profiles from a thermal analysis of the capsule using appropriate terminal sterilization chamber parameters.

Table 1. CSAD sterilization tests

Parameters	Dummy run	Lander (phase 1)	CSAD feasibility model (phase 2)
Objective	To gain experience in operations associated with performance of system level sterilization tests	To subject lander to sterilization environment that is at least as severe as cycle that lander would experience if it were in system configuration	To subject feasibility model to terminal sterilization environment that has been determined sufficient to achieve appropriate probability of survival
Configuration	Sterilization canister only	Feasibility model lander, including the impact limiter	CSAD model encapsulated in its sterilization canister mounted on handling fixture (Fig. 5)
Requirements:			
GN_2 backfill	Required	Required	Required
O_2 concentration in terminal sterilization chamber before beginning cycle	Within practical limitations	Less than 2.5%	Less than 2.5% after chamber fan mixing
O_2 concentration in canister during cycle	2% or less	Not applicable	2% or less
Chamber temperature profile, objective:	(Fig. 8)	(Fig. 8)	(Fig. 8)
Heating and cooling rate	11 ± 4°C/h	11 ± 4°C/h	11 ± 4°C/h
Maximum temperature	125 ± 2°C	125 ± 2°C	125 ± 2°C
Time at temperature	Nominal duration	16.6 h	Determined during cycle
Instrumentation:			
Number of thermocouples	21 (see Table 2)	15 (see Table 2)	59 (see Table 2)
Other	Differential pressure transducer (evacuation), oxygen analyser	None	Differential pressure transducer (evacuation), oxygen analyser
Time in terminal sterilization chamber at 125°C	27 h	16.6 h	16 h
High-low temperature test performed	Yes (see Fig. 9 for requirement)	No	No
Facilities:			
GN_2 backfill	Building 150, 25-ft simulator	Building 144, 30 x 50-in. vacuum chamber	Building 150, 25-ft simulator
Sterilization	Terminal sterilization chamber	Building 144, temperature chamber	Terminal sterilization chamber

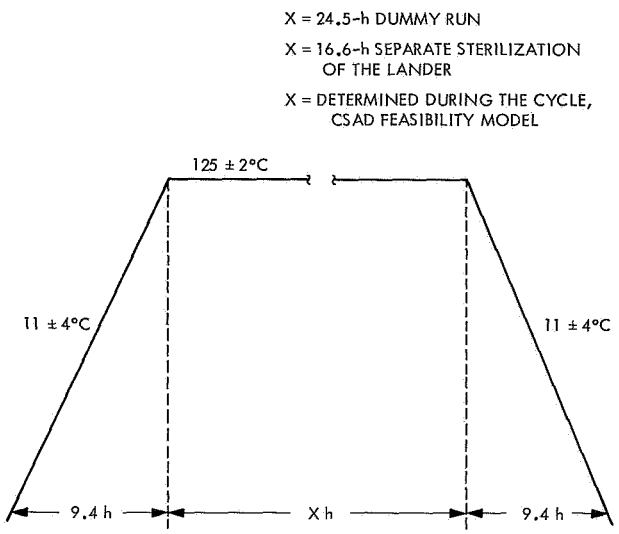

Fig. 8. Control objective, CSAD sterilization tests

(2) The probability of survival that must be achieved at the end of the cycle.

(3) The microbial heat-resistance characteristics.

(4) The number and distribution of microorganisms present at the time of capsule sterilization.

The details of the thermal analysis are covered in Subsection IV-A. The manner in which the other inputs were derived for the CSAD sterilization is discussed subsequently in the *a priori* process calculations, Subsection IV-B.

For the purposes of the process calculations, the CSAD feasibility model was divided into ten major assembly zones:

(1) Sterilization canister.

(2) Aeroshell.

(3) Relay antenna.

(4) Radiometer.

(5) Mass spectrometer.

(6) Entry package.

(7) Lander.

(8) Parachute subsystem.

(9) Deflection motor and spin-despin subsystem.

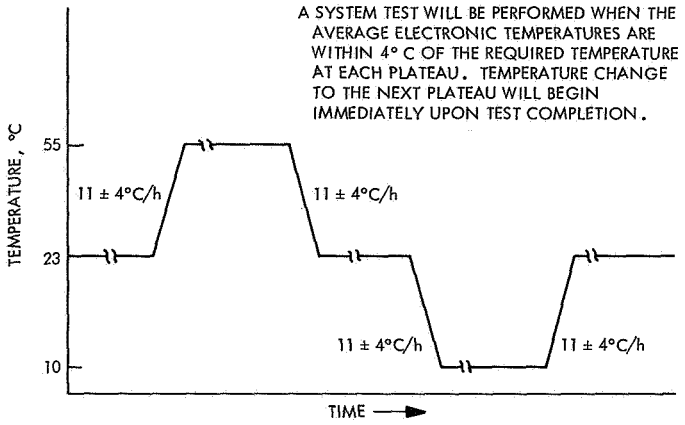

Fig. 9. Control objective high-low temperature tests, dummy run

(10) Mechanical devices and associated pyrotechnics, supports and trusses, and interconnecting cabling of major subsystems.

A. Thermal Analysis

During the program, a computer thermal model of CSAD was constructed (Fig. 10). The thermal model consisted of 72 thermal nodes in the capsule, 4 nodes for N_2 gas inside the canister, and 6 nodes for the sterilization canister. The temperature profiles of principal interest were those associated with surfaces and interiors of the major assembly zones. The structural members between the major assembly zones were not included in the analysis because of their low thermal capacitances.

1. Assumptions. The following assumptions were used for the thermal analysis.

(1) Radiative heat transfer inside the sterilization canister was assumed to be negligible. Since very small temperature differences were expected between the surfaces of the CSAD assemblies, and since the sterilization temperatures were relatively low from a radiative transfer viewpoint, the amount of heat energy transferred by the radiative mechanism would be inconsequential.

(2) For the assemblies, only internal heat conduction was considered. Heat conduction between assemblies through structural members was disregarded because large thermal gradients between different assemblies were not expected. Even if some thermal gradient existed, only a small amount of heat would be transferred through the structural members because of small cross-sectional area.

Table 2. Number of thermocouples for CSAD major assembly zones

Zone	Subzones	Subzone surface classification	Number of thermocouples		
			Dummy run	Lander (phase 1)	CSAD feasibility model (phase 2)
1. Sterilization canister	Forward section, inside surface	Exposed	5	—	5
	Aft section, inside surface	Exposed	14	—	14
2. Aeroshell	Subsystem side	Exposed	—	—	3
	Ablator side	Exposed	—	—	3
3. Relay antenna	Outer surface	Exposed	—	—	—
	Inner surface	Exposed	—	—	1
4. Radiometer		Exposed	—	—	1
5. Mass spectrometer		Exposed	—	—	4
6. Entry package	Entry chassis, outside surface	Exposed	—	—	4
	Entry chassis, inside surface	Mated	—	—	1
	Entry truss (32 struts)	Exposed	—	—	—
	Lander support structure	Exposed	—	—	—
	Entry modules	Mated	—	—	2
	Harness and connectors	Mated	—	—	—
	Aft cover, Inside surface	Mated	—	—	—
	Aft cover, Outside surface	Exposed			
	Forward cover, Inside surface	Mated	—	—	—
	Forward cover, Outside surface	Exposed			
7. Lander	Lander chassis	Mated	—	7	2
	Impact limiter, outside surface	Exposed	—	2	2
	Lander modules and battery	Mated	—	4	1
	Harness and connectors	Mated	—	1	—
	Bottom cover, Inside surface	Mated	—	—	—
	Bottom cover, Outside surface	Exposed			1
	Forward cover, Inside surface	Mated	—	—	—
	Forward cover, Outside surface	Exposed			1
8. Parachute subsystem	Canister, Inside surface	Mated	—	—	1
	Canister, Outside surface	Exposed			4
9. Deflection motor and spin-despin subsystem	Motor and truss	Exposed	—	—	2
	Jets, tubing, and valves	Exposed	—	—	—
	Gas bottles	Exposed	—	—	2
10. Mechanical devices and associated pyrotechnics, supports and trusses, and interconnecting cabling of major subsystems	Interconnecting cabling and pyroharness	Exposed	—	—	—
	Separation devices	Exposed	—	—	3

Table 2 (contd)

Zone	Subzones	Subzone surface classification	Number of thermocouples		
			Dummy run	Lander (phase 1)	CSAD feasibility model (phase 2)
Other thermocouples[a]			2	1	2
Total on capsule			19	14	57
Total used for test			21	15	59

[a]Including chamber temperature and CSAD handling fixture temperature.

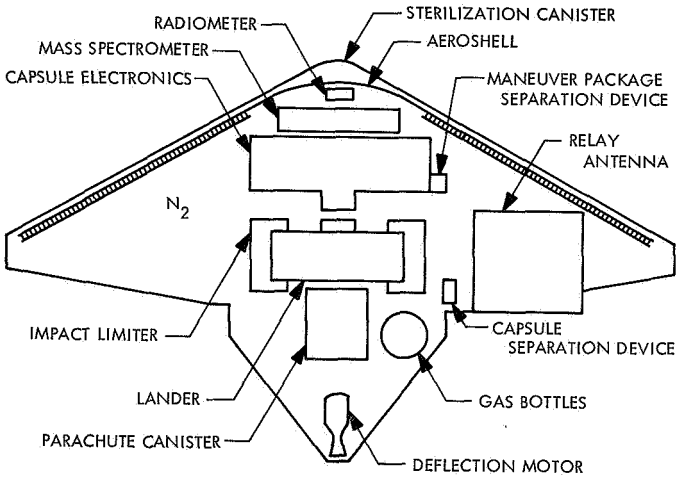

Fig. 10. Analytical thermal model

(3) All assemblies and materials were assumed to be homogeneous relative to thermal properties. The assumed average value of the thermal properties of various materials is given in Table 3. The assumed densities of the assemblies are given in Table 4. All science instruments were assumed to have the same thermal properties: a thermal conductivity of 1.2 Btu/h-ft-°F and a heat capacity of 0.2 Btu/lb-°F. The interior of the parachute canister was assumed to be solid nylon for one model, and alternating layers of nylon and air for the conservative model. The impact limiter was assumed to be solid balsa wood.

(4) An internal free convection heat transfer coefficient of 1.0 Btu/h-ft^2-°F was assumed. The gas inside the sterilization canister was nitrogen. This gas was selected to minimize oxidation.

Table 3. Thermal properties

Material	Thermal conductivity, Btu/h-ft-°F	Heat capacity, Btu/lb-°F	Density, lb/ft^3
Aluminum	100.0	0.19	175.0
Balsa wood	0.0275	0.3	7.5
Beryllium	87.0	0.1	500.0
Fiberglas honeycomb	0.11	0.23	4.0
Silicone elastomer	0.052	0.36	42.5
Nitrogen	0.017	0.24	0.06
Nylon parachute	0.12	0.35	29.4
Steel	14.4	0.14	484.0

Table 4. Density of components

Assembly	Density, lb/ft^3
Sterilization canister	175.0
Aeroshell	4.0
Radiometer	120.0
Mass spectrometer	43.0
Capsule electronics	67.0
Maneuver package separation device	127.0
Impact limiter	7.5
Lander	81.0
Capsule separation device	172.0
Relay antenna	8.0
Parachute canister	29.4
Gas bottles	175.0
Deflection motor	484.0

(5) The sterilization canister driving temperature profile was assumed to be identical to that of the terminal sterilization chamber.

(6) The initial temperature of the entire capsule was at room temperature, 23°C.

2. Sterilization approaches and boundary conditions. In an attempt to optimize the sterilization cycle, two possible approaches were considered:

(1) The sterilization canister would be heated and cooled in the terminal sterilization chamber by convection of the nitrogen gas. Since it was assumed that the canister temperature profile would follow the chamber profile, the capsule assemblies would be heated and cooled by convection and conduction through the nitrogen gas within the canister. To determine the resultant assembly temperature profiles, thermal analyses were performed using chamber heating and cooling rates of 11°C/h (case 1) and of 19, 25, and 40°C/h (case 2). A rate of 40°C/h was believed to be the maximum capability of the chamber. The process calculations based on these profiles are discussed in Section IV.

(2) The second approach would be to circulate preheated (precooled for cooling) nitrogen gas into the canister. This method would increase the rate of heat transfer into each assembly from the internal gas. (The two most important parameters in determining the assembly temperature profiles were the thermal properties of the individual assemblies and the temperature profile of the internal gas. Since the thermal properties of the assemblies could not be significantly changed, the major effort in reducing the heating time involved changing the internal gas temperature profile.) A thermal analysis was performed by assuming that preheated nitrogen gas at 125°C was circulated into the canister until the capsule had reached 125 ± 1°C; then nitrogen gas at 23°C was circulated for the cool-down (case 3). Since this assumption could result in thermal shock damage to structural members, an additional thermal analysis was performed assuming that the nitrogen gas inside the canister had a heating and cooling rate of 11°C/h rather than starting instantaneously at 125°C (case 4).

Using the boundary conditions shown in Fig. 11, the first analytical model was exercised to determine the difference in response characteristics and cycle time at each major assembly zone. For graphical comparison, the temperature profiles of the parachute canister surface, the center of the lander, and the center of the entry electronics are presented for both approaches in Fig. 12. These predictions were used to determine the sensitivity of process duration to various heating and cooling conditions. These analytical results are discussed at the end of this section.

The parachute canister was bolted to the lander with an air gap between the bottom surface of the canister

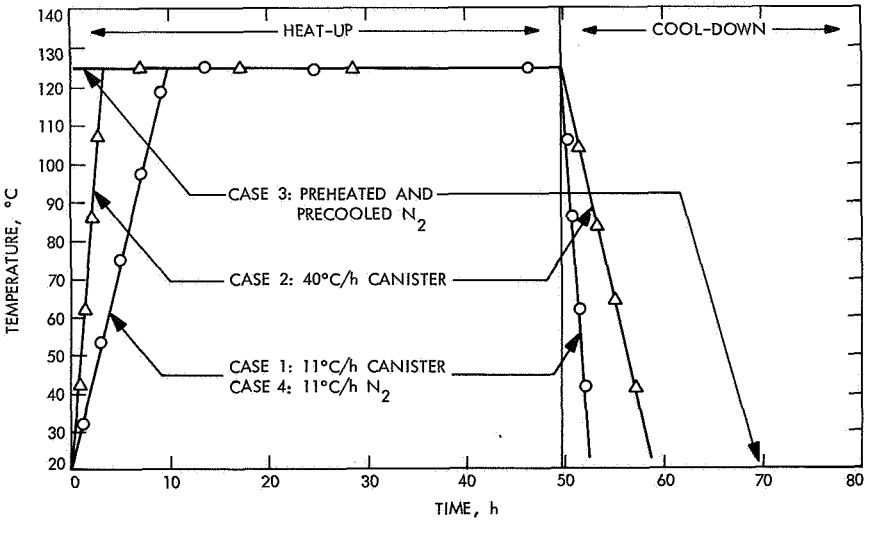

Fig. 11. Boundary conditions for temperature profiles

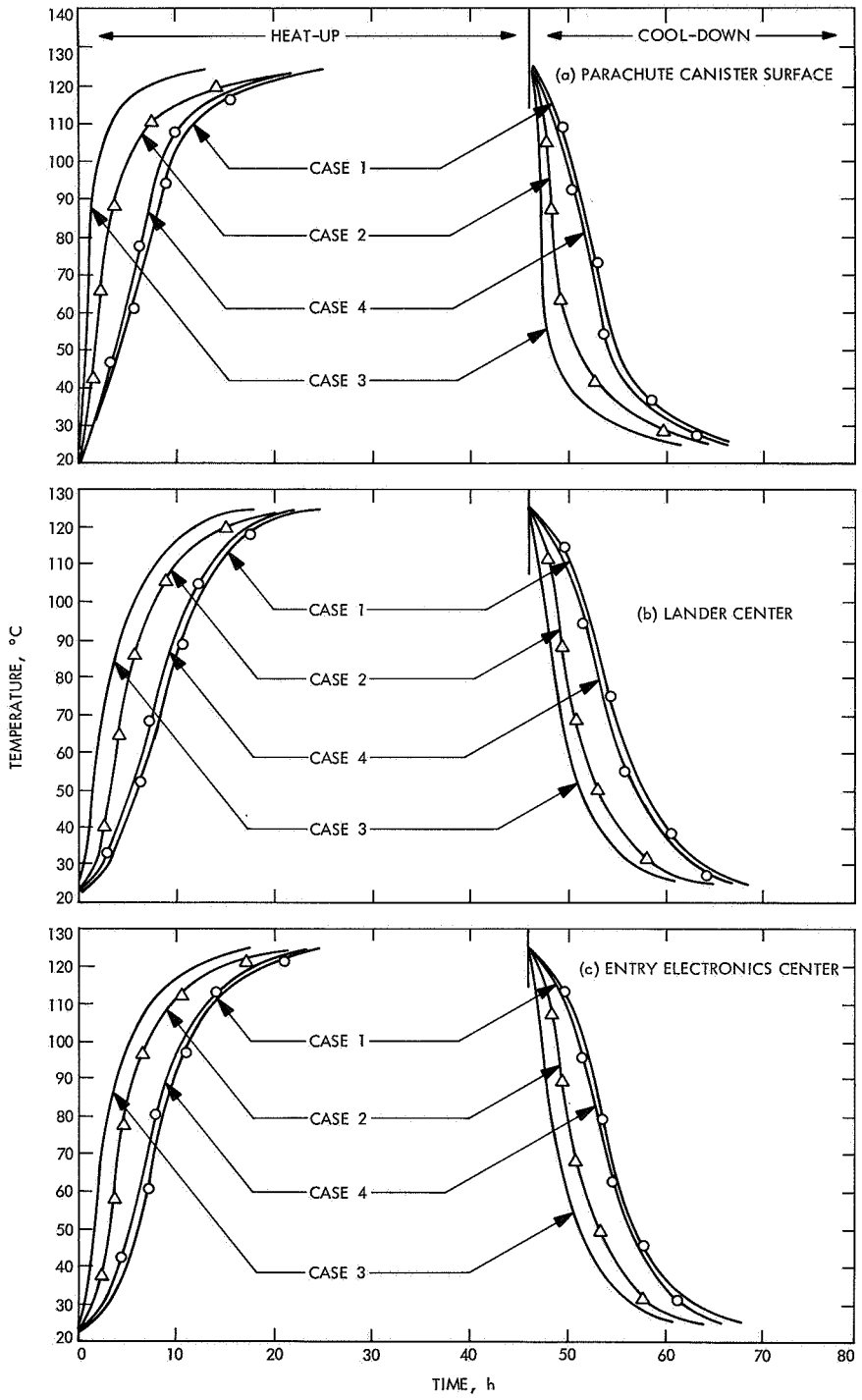

Fig. 12. Temperature profiles

and the lander (Fig. 13) for the phase 2 terminal sterilization test. Since this construction could significantly affect the temperature responses of these two major assembly zones, the second thermal model of the capsule was constructed with the two zones directly coupled. This one was a conservative model that coupled the parachute and lander thermally and modified the parachute heat transfer coefficients. The purpose of the profiles from the conservative model was to provide a predicted temperature profile above which all temperature responses measured during the sterilization cycle would lie.

The predictions for a family of heating profiles for both the first thermal model and the conservative model are shown in Fig. 14. It was anticipated that all temperature responses measured during the sterilization cycle would lie between the terminal sterilization chamber profile and the seventh profile, which was the point of greatest thermal lag in the conservative model. This approach of bracketing a wide range of temperature responses was necessary because there had been no verification that the computer models adequately represented the thermal behavior of the CSAD feasibility model during the sterilization cycle. In a flight program, verification would be accomplished by a capsule thermal test model or proof test model prior to terminal sterilization of the flight capsule.

B. *A Priori* Process Calculations

Based on the temperature profiles generated by the thermal analysis effort, a series of process calculations

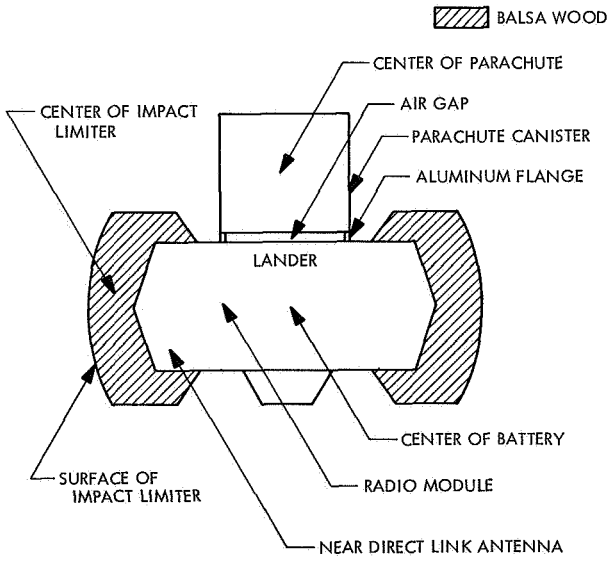

Fig. 13. Parachute-lander combination cross section

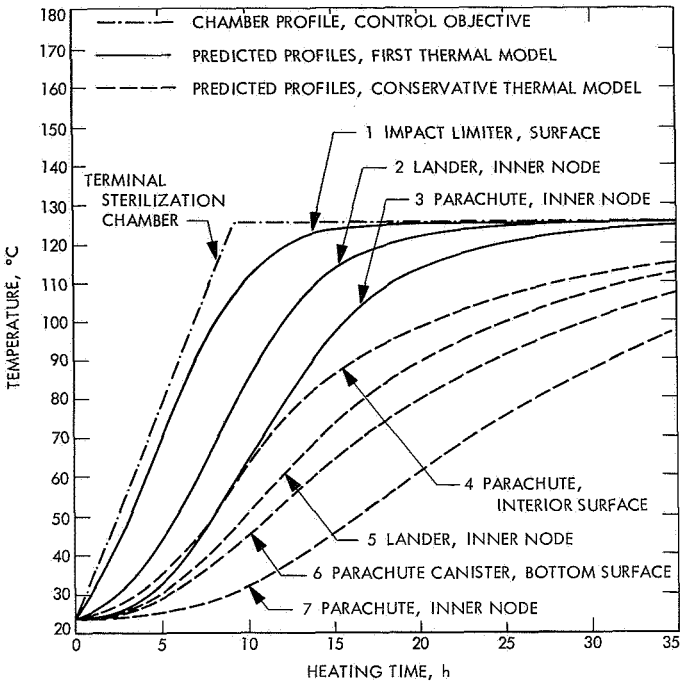

Fig. 14. Family of heating profiles

were performed in an attempt to optimize the sterilization process for the CSAD feasibility model. The objectives of the *a priori* process calculations were:

(1) To minimize the duration of the sterilization cycle by evaluating the effects of variations in the heating and cooling rates on process times.

(2) To provide length-of-cycle alternatives for the sterilization engineer to use during the process.

It was assumed that interiors of all assembly level items were sterilized as a consequence of the subsystem sterilization tests (such as flight acceptance tests), or other specific sterilization processes (Ref. 2). For the CSAD feasibility model, some of the subsystems were subjected to a subsystem sterilization cycle; others were not. However, for the process calculations, it was assumed that all subsystems had been internally sterilized. Thus, the microbial burden on the capsule was assumed to be located in two areas: exposed surfaces and mated surfaces. The exposed surfaces were those surfaces that would be illuminated if the capsule (without the sterilization canister) were placed in the center of an inwardly directed luminous sphere (i.e., all surfaces directly in contact with the canister atmosphere). The mated surfaces included all surfaces not classified as exposed.

The probability of survival of one or more organisms on the assembled capsule was required to be 10^{-3}. Since ten major assembly zones had been defined in the capsule, and it was assumed that the survival probabilities could be uniformly distributed, the probability number for each major assembly zone becomes:

$$P_{s_{MZ}} = \frac{P_{s_{Cap}}}{n_{MZ}} = \frac{10^{-3}}{10} = 10^{-4}$$

where $P_{s_{MZ}}$ is the probability of one or more survivors in a major assembly zone, $P_{s_{Cap}}$ is the probability of survivor(s) in the capsule, and n_{MZ} is the number of major assembly zones.

For the process calculations, D values* at 125°C of 20 min, 40 min, and 3.5 h for exposed surfaces, mated surfaces, and interiors, respectively, were used. The 3.5-h D value is included in the analytical calculations for academic reasons. For all CSAD calculations, a z value* of 25°C was used.

The equivalent sterilizing time* F_T equation is the basic relationship underlying the process determination:

$$F_T = D_T \frac{\log N_o}{P_{s_{MZ}}}$$

where N_o is the number of microorganisms on a major assembly zone. This equation is sometimes expressed as

$$F_T = D_T \frac{\log N_o}{P_{s_{MZ}}} - 1 \qquad (1)$$

to account for the initial reduction, which is often encountered in the first few minutes of heating a microbial population. This form of the equation was used in calculating all CSAD process times. Thus, fixing $P_{s_{MZ}} = 10^{-4}$ and varying N_o and/or D_T, the parametric relationship between F_T, N_o, and D_T was defined.

*The term D is defined as the decimal reduction time, or the time at temperature, required to destroy 90% of the microorganisms. The term z is numerically equal to the number of degrees F (or C) required for a thermal destruction curve to traverse one log cycle (Ref. 3). The term F_T is the time in minutes required to reduce the microbial population to the desired probability of survival of one or more organisms assuming instantaneous heating and cooling (Ref. 1).

For the evaluation of the effects of variations in heating and cooling rates on process times, N_o was fixed at 10^4. The first thermal model was used.

For the determination of length-of-cycle alternatives, D_T was fixed at 40 min, and N_o was varied from 10^8 microorganisms to 1 microorganism. Temperature profiles from the first thermal model and the conservative model were used (Fig. 14).

C. Analytical Results

Process times resulting from the variation of heating and cooling rates are shown in Table 5. The maximum temperature is that temperature occurring on the particular item at the end of the heat application portion of the cycle. However, the maximum temperature of the terminal sterilization chamber (125°C) did not have to be achieved at each location in order to accomplish sterilization of the major assembly zone. For example, for 11°C/h heating and cooling rate, the maximum temperature is 118°C and the time of heat application is 13.5 h. Since it takes 9.4 h to bring the chamber to 125°C, the time that the chamber is at 125°C is only 4 h. The time required to cool the aeroshell surface from 118 to 25°C is 18.5 h. The total process time from 23°C to a maximum temperature to 25°C is 32 h. (The time that a particular item achieved the 25°C was chosen as the temperature of the cycle, because to return to the initial temperature of 23°C an additional 5 or 6 h of cooling would be required.)

The reduction in heat application time as compared to the 11°C/h rate is shown in Table 6. Case 3 is the forced convection condition where the atmosphere inside the canister is instantaneously at 125°C for heating and at 25°C for cooling. This case was included to show the theoretical minimum value for heat application time. This condition would probably result in damage to structural members caused by differential expansion, hence, should be excluded from further consideration. The range of process time reduction is from 1.9 h to 4.5 h, if case 3 is excluded. From a sterilization point of view, changes of these magnitudes are not considered significant. The heat application times on the center node of the lander range from 20 to 17 h by varying the heating and cooling rate from 11 to 40°C. Based on these analyses and the fact that the possible structural deformation could occur during the 25 and 40°C/h processes plus the concern that past development work on materials and hardware would be invalidated if a higher rate were chosen, the 11°C/h rate was recommended.

Table 5. CSAD process times for different heating and cooling rates[a]

Location	Analysis case, rate						
	1, 11°C/h	2, 19°C/h	2, 25°C/h	2, 40°C/h	3[b]	4[c]	Assumed[d]
Aeroshell, surface							
Maximum temperature, °C	118	118	119	118	120	120	
Heat application, h	13.5	11.2	10.7	9.0	6.0	11.6	20 min
Chamber at 125°C, h	4.1	5.8	6.6	6.4	(6.0)[e]	(2.21)[e]	
Total process, h	32.0	27.2	29.9[f]	25.4	16.0	25.6	
Parachute, canister surface							
Maximum temperature, °C	117	118	117	117	118	118	
Heat application, h	14.7	12.8	12.0	11.0	9.5	13.7	20 min
Chamber at 125°C, h	5.3	7.4	7.9	8.4	(9.5)	(4.3)	
Total process, h	36.0	32.7	31.0[f]	29.5	24.5	32.3	
Lander, inner node							
Maximum temperature, °C	122	122	122	122	122	122	
Heat application, h	20.0	18.0	17.5	17.0	14.0	19.2	40 min
Chamber at 125°C, h	10.6	12.6	13.4	14.4	(14.0)	(9.8)	
Total process, h	40.9	36.5	35.8[f]	35.1	29.0	37.5	
Interior node							
Maximum temperature, °C	125	125	125	125	125	125	
Heat application, h	44.8	43.8	43.3	42.6	40.8	43.8	3.5 h
Chamber at 125°C, h	35.4	38.4	39.2	40.0	(40.8)	(34.4)	
Total process, h	74.5	73.5	68.2	67.7	65.8	73.6	

[a]Lethality calculation assumptions: $N_0 = 10^4$ microorganisms, $P_s = 10^{-4}$, $Z = 25$°C, and lethality begins at 100°C.

[b]Case 3 at forced convection condition of hot gas at 125°C and cooling gas at 23°C.

[c]Case 4 at forced convection condition of gas following a 11°C/h rate.

[d]Process times associated with D values assumed at 125°C.

[e]Bracketed number is the time that canister atmosphere would be at 125°C.

[f]Estimated, cooling profile not complete.

Table 6. Reduction in heat application time relative to analysis case 1

Location	Analysis case, rate				
	2, 19°C/h	2, 25°C/h	2, 40°C/h	3[a]	4[b]
Aeroshell, surface, h	2.3	2.8	4.5	7.5	1.9
Parachute canister, surface, h	1.9	2.7	3.7	5.2	1.0
Lander, inner node, h	2.0	2.5	3.0	6.0	0.8
Interior node, h	1.0	1.5	2.2	4.0	1.0

[a]Forced convection condition of hot gas at 125°C and cooling gas at 23°C.

[b]Forced convection condition of gas following a 11°C/h rate.

The following observations (based on the CSAD configuration) can be made from Table 5:

(1) As the heating rate increases, the heat application time decreases (as expected), but the time the terminal sterilization chamber needed to be at 125°C increases. This is attributed to the larger lethality occurring during the transient phases for the cycles with slow heating and cooling rates. If the time a subsystem is at 125°C can be used as a measure of severity, a subsystem with low thermal mass (such as the radiometer) would experience a more severe sterilization environment at the 40°C/h rate than at the 11°C/h rate, even though the same sterility level is achieved.

(2) There is no significant reduction in heat application time between having the canister heated and cooled in the chamber by convection of nitrogen gas (approach 1, case 1) or by forcing hot gas through the canister (approach 2, case 4). There would be implementation difficulties in using the forced convection mode, such as the limitation on flow rate imposed by the maximum rate tolerable through the biological filter, possible tearing or damage of thermal shields, and possible damage caused by large thermal gradients between assemblies.

Craven, Stern, and Ervin (Ref. 2) noted that the process duration for the system sterilization is determined by the process times associated with the mated surfaces. The same conclusion was drawn early in the CSAD analytical studies when the D values at 125°C were varied and all other parameters including temperature profiles were fixed. The process times resulting from the variation of D values is shown in Table 7. As noted previously, the process times associated with the D value at 125°C of 3.5 h are included for academic reasons. If there is an identical number of microorganisms on the exposed surface of a given major assembly zone and on the mated surface of the same (or different) major assembly zone, and both surfaces follow the same temperature profile (e.g., profile 3), the exposed surface would be sterilized in less time (36.6 h) than the mated surface (40.3 h). This lower sterilization time occurs because of slower temperature response and greater microbial heat resistance on the mated surfaces than on the exposed surfaces. Thus, the sterilization cycle applied to the capsule would be determined from the heat application times associated with the mated surfaces of the major assembly zones.

To ensure conservatism in the process calculations associated with the determination of the length-of-cycle alternatives, it was assumed that the microbial burden on the mated surfaces of a given major assembly zone would be concentrated at the mated surface of that zone with the greatest thermal lag. Thus, to achieve sterility of the zone, the mated surface microbial burdens needed to be reduced to the appropriate survival probability.

Table 7. CSAD process times for different D values at 125°C[a]

Maximum temperature, °C	Heat Application,[b] h	Cooling,[c] h	Total process,[d] h
Exposed surface			
120	12.0	14.4	26.4
117	15.0	20.3	35.3
118	17.4	19.2	36.6
116	22.3	25.3	47.6
Mated surface			
123	15.2	14.5	29.7
121	18.7	20.9	39.6
121	20.3	20.0	40.3
120	26.0	26.0	52.0
Interior			
125	35.7	15.0	50.7
125	39.7	22.0	61.7
125	39.9	22.0	61.9
125	45.0	30.0	75.0

[a]Lethality calculation assumptions: $N_o = 10^4$ microorganisms; $P_s = 10^{-4}$; $D_{125°C} = 20$ min (exposed surfaces) = 40 min (mated surfaces) = 3.5 h (interiors); $Z = 25°C$; and lethality begins at 100°C. Heating and cooling rate = 11°C/h.

[b]Heat application is the time from 23°C to maximum temperature.

[c]Cooling is the time from maximum temperature to 25°C.

[d]Total process is the sum of heat application and cooling.

If the N_o in Eq. (1) is redefined to be N_{o_m} (the number of microorganisms on all mated surfaces of a major assembly zone) and is varied from 10^8 to 1, and $P_{s_{MZ}} = 10^{-4}$ and $D_{125°C} = 40$ min are fixed values, then a parametric relationship between F_T and N_{o_m} is defined.

Since the temperature profile of the mated surface with the greatest thermal lag could lie somewhere between the terminal sterilization chamber profile and profile 7 of Fig. 14, process calculations for each of the profiles and each value of N_{o_m} were performed. These calculations resulted in heat application and total process times for

each profile-microbial reduction combination. The heat application time was used to generate a family of parametric curves that could be correlated with a chamber parameter easily adjusted during the sterilization. The time of chamber heating from ambient to required temperature (125°C) was subtracted from the heat application time to calculate the chamber time at temperature. The results of the process calculations are shown in Fig. 15, where the microbial reduction is related to corresponding chamber time at temperature.

An example of the technique for selecting a length-of-cycle alternative is given in the following. Suppose the temperature measurement of the mated surface with the greatest thermal lag of a given major assembly zone (e.g., the lander) is between predicted profiles 4 and 5 (or on 5) of Fig. 14. Further, suppose N_{o_m} for the lander is 2400 microorganisms. Then, to be conservative, since the temperature measurement is between 4 and 5, the parametric curve associated with profile 5 is selected. Thus, the microbial reduction from Eq. (1) is

$$\frac{F_T}{D_T} = [\log(2400) - \log(10^{-4})] - 1$$
$$= 3.38 + 4 - 1 = 6.38$$

Thus, from Fig. 15, the time the terminal sterilization chamber would be at temperature is 29.5 h.

V. Microbiological Monitoring

The purpose of the CSAD microbiological monitoring effort was to determine an estimate of the microbial burden on the major assembly zones for the CSAD feasibility model sterilization cycle and to implement the refined techniques and procedures that were derived from the *Mariner* Venus 67 Monitoring Program.* Since the process calculations assumed that all assemblies had been internally sterilized, no attempt was made to determine levels associated with interiors, or screws, bolts, and harness Ty-rap.

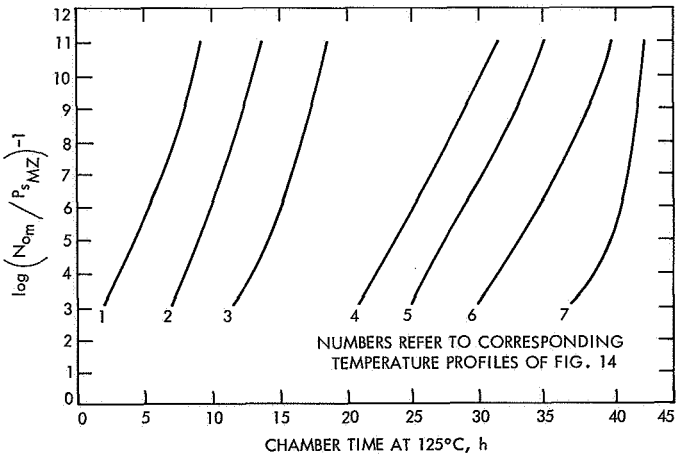

Fig. 15. Parametric curves

The CSAD monitoring program marked the first time that scheduled assays were incorporated into the test operations plan (Figs. 6 and 7). This permitted updating the microbial estimates periodically and resulted in more meaningful microbial burden numbers for the final process determinations.

A. Assembly Environment

All hardware was assembled in the southwest corner of the 80- × 120-ft high bay area of the Spacecraft Assembly Facility. Air make-up in the area (evaluated between a class 10,000 and a class 100,000 conventional clean room) was 80% internal and 20% external, with filtration by Farr HP-2 filters.

No special biological constraints were imposed during assembly, other than the personnel wearing caps, gowns, and gloves, as is normally done on a flight program. Prior to its immediate need, all CSAD hardware was kept in closed containers within the quality assurance bonded stores, and assembled capsule packages were covered with a decontaminated plastic nonstatic sheet at the end of the working day.

B. Assay Methods and Procedures

The methods recommended in the NASA standard procedures for microbial assay of spacecraft hardware (Ref. 4) are stainless steel settling strips and swab-rinse techniques. The latter method was used because of the problems associated with the adaptation of the strip techniques to the assembly and testing of a flight vehicle.

Although problems were also encountered with swab-rinse techniques, specific revisions made this method the best choice for capsule burden determinations. The revisions limited the assay to enumeration of heat resistance

*Christensen, M. R., Green, R. H., and Stern, J. A., *Microbiological Monitoring of the Mariner V Spacecraft*, Section Report 604-54. Jet Propulsion Laboratory, Pasadena, Calif., July 10, 1969.

aerobic spore-forming microorganisms, and eliminated division (aliquots) of the sample since the entire sample was analyzed.

Sterile cotton tipped swabs were moistened in 0.1% peptone broth, the test site was sampled, and the swab head was aseptically detached into the peptone. Following insonation (25 kHz for 12 min) the samples were heat shocked for 18 min at 80°C. The entire sample was then pipetted into Petri plates and covered with molten agar. Five ml of sterile peptone was aseptically added to the tube containing the swab head, and all samples were incubated at 32°C for 72 h. Microbial growth was reported as viable spores per 4 in.^{2} of swabbed surface and appropriate sterility controls were utilized to denote contaminants.

C. Microbiological Monitoring Approach

A large portion of the samples assayed during the *Mariner* Venus 67 program yielded zero counts. Such data imposed limitations upon the statistical approaches available for analysis. To alleviate this problem, it was decided to sample a minimum of 10% of each major assembly zone. Depending upon their complexity, major zones were further divided into subzone areas, with the 10% minimum sampling relationship being maintained. (For example, the lander chassis was partitioned into 188 subzones, representing horizontal, vertical, and inclined areas.) The capsule was further delineated into mated and exposed areas under the rationale presented earlier. (Figure 16 includes the zone and subzone sampling ratios, as well as the mated and exposed area percentages.) Of the 417-ft^2 surface area of the capsule system, 356 ft^2 was designated as exposed and 61 ft^2 was classified as mated.

All samples were collected in the high bay area, except for the modules and instruments (see Table 8 for typical module breakdown), which were sampled within a class 100 laminar flow bench prior to their insertion into the capsule. To minimize handling contaminants, microbiological personnel wore caps, gowns, and sterile surgical gloves.

All structures and components on the capsule system were sampled except for the interconnect harness, pyro-harness, and the batteries. For the harnesses, an average spore burden value per unit length was derived from assay of typical flight harness cable and connector. By enumerating the number and length of cables and connectors in a harness, and extrapolating the mean burden to them, a burden value for the harness was determined. The battery burden was determined by sampling an adjacent area to the battery support structure, and projecting that burden to the battery.

D. Microbiological Monitoring Results

For the purposes of capsule burden estimates, it was assumed that:

(1) The burden associated with the harness and connectors remained constant once determined.

(2) No increase or die-off of microbial numbers occurred at mated areas once modules were inserted.

Table 8. Spore burden, lander modules

Lander modules	Reference designation	Function[a] on feasibility model	Microbial burden estimates
Radio			
Transmitter	52A0	FF	6
	52A1	FF	4
	52A2	FF	10
	52A3	FF	0
RF isolator	52A4	PF	5
Six pole RF switch	52A5	PF	4
RF cables		FF	2
Power			
Control unit	54A1	FF	13
Batteries	54A2	FF	29
Sequencer and timer	55A1	FF	25
Data handling	56A1	NFMU	13
Chemical heater	61A1	NFMU	11
Mechanical devices			
Instrument booms	62A1	FF	90[b]
	62A2	FF	8
Landing sensor	62A3	FF	5
Science			
Wind instrument	75A1	FF	NS[c]
Gas chromatograph	76A1	NFMU	NS
TOTAL			225

[a]FF = Fully functional, mechanically/electrically; PF = Partly functional electrically, mechanically similar to flight design in shape, size, and structural material; NFMU = Nonfunctional mockup which is mechanically similar to flight design in weight, shape, size and structural material.

[b]Possible contamination.

[c]Not available for sampling.

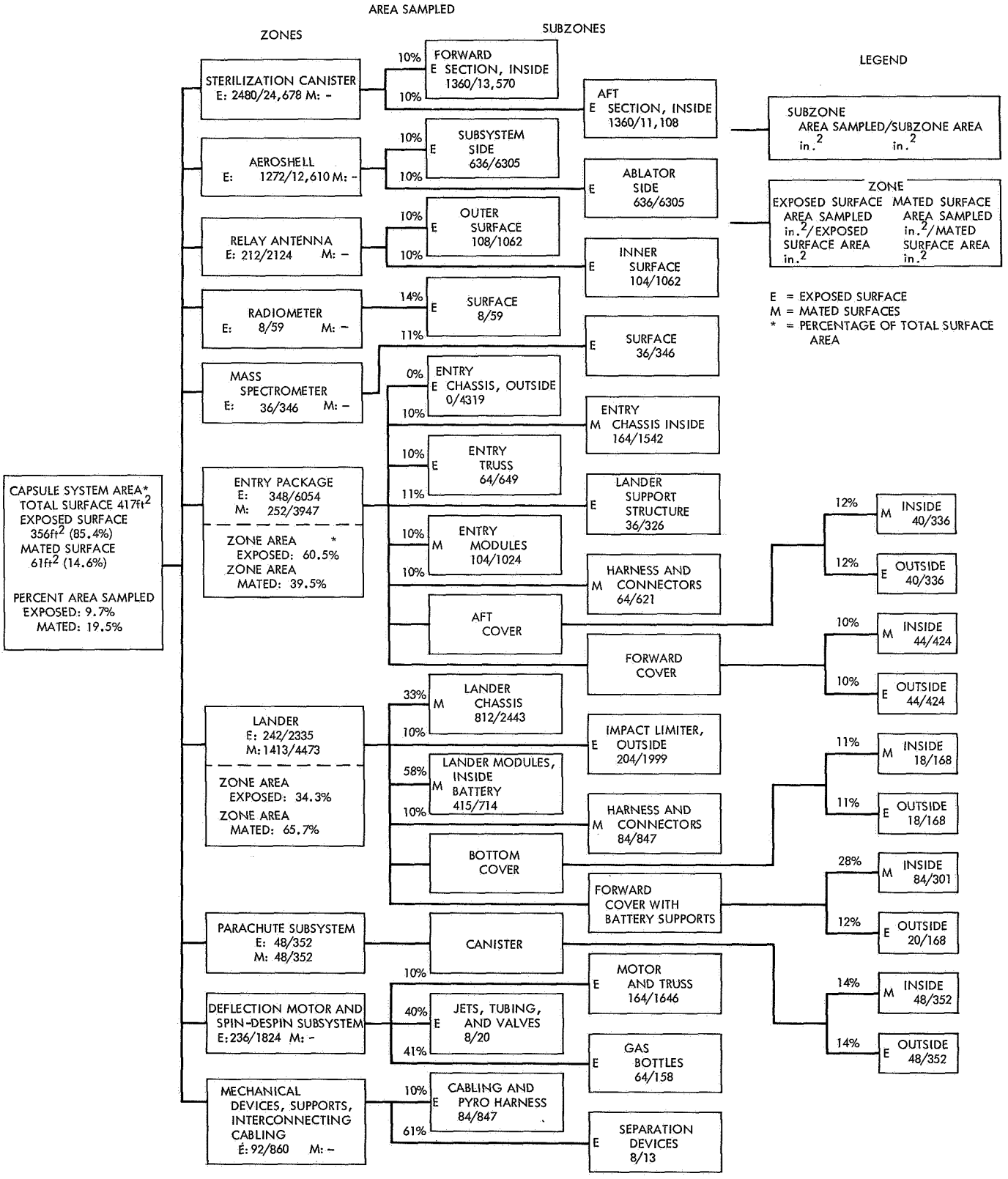

Fig. 16. CSAD microbiological monitoring

(3) The most recent data obtained from a test site would be used.

(4) Swab recovery efficiency was a conservative 30%.*

(A correctional multiplicative factor of 3.33 was applied to all data.)

Final pre-sterilization capsule estimates are presented in Table 9. For the lander, the total spore burden was 9367 spores with only 1635 on the mated surfaces. Most of the lander burden was located on the balsa impact limiter. Other than the limiter, the highest source of microbial spores was the ablator material (silicone elastomer base) on the aeroshell. Total capsule spore burden was estimated to be 5.3×10^4, of which 4973 spores were in mated areas, with the remainder on exposed surfaces.

In summation, the 10% zonal sampling approach resulted in better burden estimates than had resulted from previous spacecraft microbial monitoring programs. The reason was that the effect of sampling and enumeration errors on the results was minimized by increasing the area sampled and by zoning the capsule, which together decreased the area extrapolation factors resulting in less sensitivity to errors. The zonal sampling approach would be a feasible technique for determining spacecraft burden levels on future spacecraft sampling programs.

VI. Sterilization Test Results

The following discussion presents the results of the three system-level sterilization tests, which were summarized in Table 1 of Section III.

A. Dummy Run

The oxygen preconditioning portion of the test demonstrated the plausibility of the technique of backfilling the canister in one location and sterilizing in another without a large increase in oxygen concentration during the transportation period. Although the results were encouraging, they were not conclusive because of instrumentation difficulties.

The oxygen concentration measurements during the test indicated that continuous purging would be required and no weekend or overnight shutdown of the purging could be tolerated if the oxygen level were to be maintained below 2%.

The assumption that, for the computer thermal model, the sterilization canister temperature profile is equivalent to terminal sterilization chamber profile was verified during the dummy run.

The low temperature for the pre- and post-sterilization tests (Fig. 17) could not be achieved, because of facility limitation (not designed for such an operation).

The high-temperature tests and the sterilization cycle were nominal (Figs. 18 and 19). The time that the chamber was at 125°C for the sterilization test was 27 h.

B. Separate Sterilization of the Lander

The separate sterilization of the lander was representative of an engineering heat sterilization test on a subsystem because the sterilization environment was as severe as the cycle that the lander would experience if it were in the system configuration.

The oxygen preconditioning and the sterilization cycle were successfully completed with all test requirements satisfied. The temperature responses were as predicted, as shown in Fig. 20.

The visual inspection after the test indicated that the string ties on the cables had discolored and microcracks appeared in some of the RF connectors.

The lander sequencer and timer failed in a post-sterilization lander functional test. The problem was later attributed to poor workmanship on a counter stage terminal.

C. CSAD Feasibility Model Sterilization

The sequence of events during the CSAD feasibility model sterilization test is given in Table 10. The entire operation was performed without difficulty.

As noted in Section III and Table 10, the first step in the sterilization test is the evacuation of the atmosphere in the capsule and the backfilling with an inert gas to minimize the possibility of oxidation of materials. Since the terminal sterilization chamber has no vacuum capability, this operation was accomplished in a nearby

*Various investigators (Ref. 5) have determined swab recovery efficiency to be between 35 and 40%.

Table 9. Estimated spore burden for CSAD major assembly zones[a]

Zone	Subzones	Subzone surface classification	Subzone estimate	Zone-mated surface estimate	Zone-exposed surface estimate	Total zone estimate
1. Sterilization canister	Forward section, inside surface	Exposed	5,750	—	10,673	10,673
	Aft section, inside surface	Exposed	4,923			
2. Aeroshell	Subsystem side	Exposed	4,956	—	20,832	20,832
	Ablator side	Exposed	15,876			
3. Relay antenna	Outer surface	Exposed	633	—	866	866
	Inner surface	Exposed	233			
4. Radiometer		Exposed	50	—	50	50
5. Mass spectrometer		Exposed	270	—	270	270
6. Entry package	Entry chassis, outside surface	Exposed	1,094	—	833	833
	Entry chassis, inside surface	Mated	833			
	Entry truss (32 struts)	Exposed	410	2,992	2,934	5,926
	Lander support structure	Exposed	240			
	Entry modules	Mated	643			
	Harness and connectors	Mated	1,376			
	Aft cover, Inside surface	Mated	80			
	Aft cover, Outside surface	Exposed	760			
	Forward cover, Inside surface	Mated	60			
	Forward cover, Outside surface	Exposed	430			
7. Lander	Lander chassis	Mated	673	1,635	7,732	9,367
	Impact limiter, outside surface	Exposed	7,440			
	Lander modules and battery	Mated	450			
	Harness and connectors	Mated	373			
	Bottom cover, Inside surface	Mated	113			
	Bottom cover, Outside surface	Exposed	266			
	Forward cover, Inside surface	Mated	26			
	Forward cover, Outside surface	Exposed	26			
8. Parachute subsystem	Canister, Inside surface	Mated	346	346	570	916
	Canister, Outside surface	Exposed	570			
9. Deflection motor and spin-despin subsystem	Motor and truss	Exposed	100	—	276	276
	Jets, tubing, and valves	Exposed	20			
	Gas bottles	Exposed	156			
10. Mechanical devices and associated pyrotechnics, supports and trusses, and interconnecting cabling of major subsystems	Interconnecting cabling and pyroharness	Exposed	3,636	—	3,752	3,752
	Separation devices	Exposed	116			
CSAD totals				4,973	47,955	52,928

[a]Data includes a 30% efficiency factor.

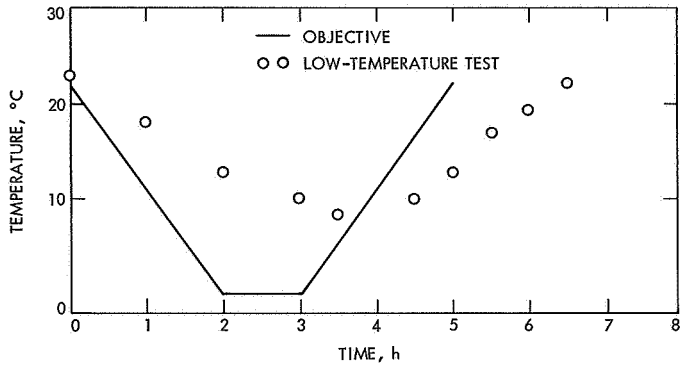

Fig. 17. Control profile, low-temperature tests, dummy run

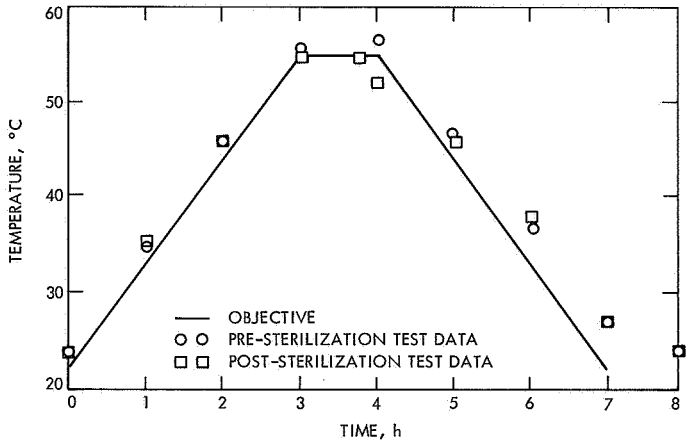

Fig. 18. Control profile, high-temperature tests, dummy run

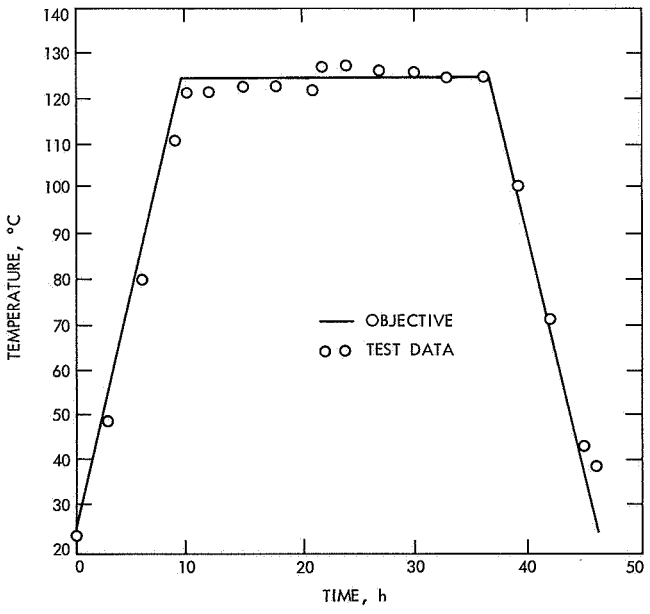

Fig. 19. Control profile, sterilization cycle, dummy run

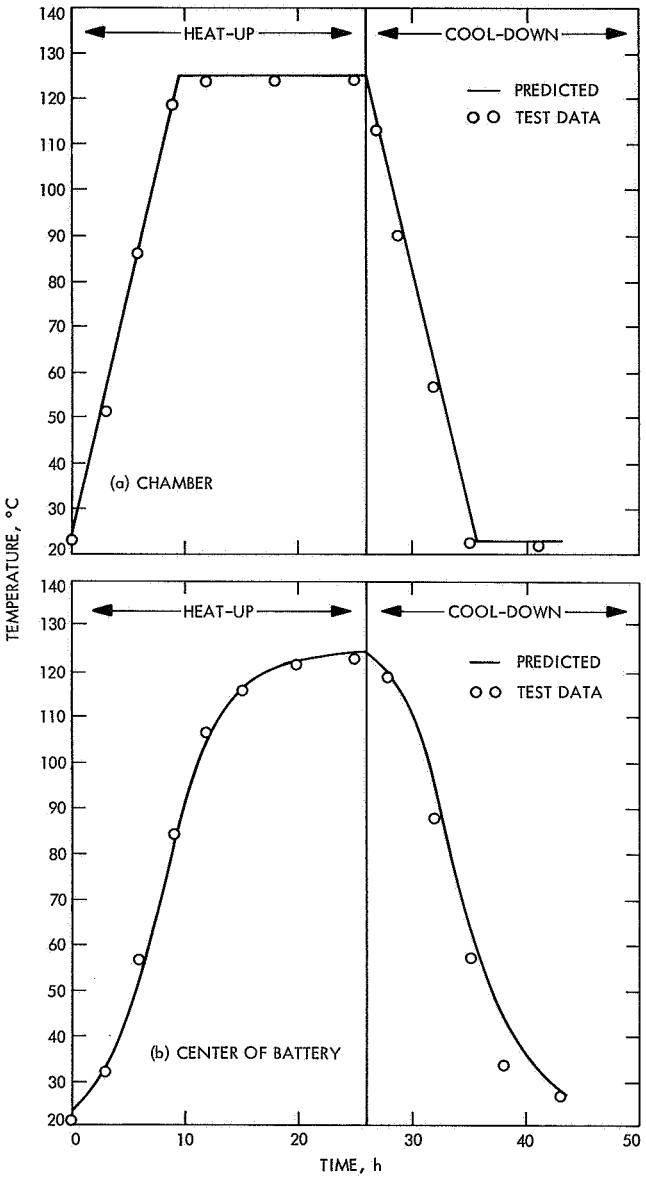

Fig. 20. Temperature profiles, predicted vs actual, separate sterilization of the lander chamber and center of battery

Table 10. Sequence of sterilization events on CSAD feasibility model

Event	Date, 1968	Time	Nominal time, h
Move to 25-ft space simulator	5/15	0940	
Arrive at 25-ft space simulator		1000	
Start evacuation of chamber		1128	
Pressure at 1.2×10^{-2} torr		1315	
Begin backfill		1340	
At ambient pressure		1500	
Removal of model from chamber		1515	
Sample taken of O_2 concentration		1530	
Transport model to chamber		1540	
Arrive at chamber		1616	
Sample taken of O_2 concentration		1700	
Start N_2 purge		1720	
Heating element turned on		1915	
Starting up ramp		2215	0
Oven at 125°C (±2°C)	5/16	0730	9.4
Preliminary estimate for time chamber at temperature made (16 h)		0930	10
Preliminary estimate reviewed		1420	15
Model committed to a sterilization cycle of 16 h at 125°C		1840	20
Begin cooling	5/17	0015	26
Chamber at ambient temperature		1000	35.4
Heating element turned off and GN_2 purge terminated		1415	
Turned off data system	5/18	0915	

vacuum facility. The measurements of the capsule atmosphere (Table 11), taken after backfilling in the vacuum chamber and before purging the terminal sterilization chamber, determined the relative abundance of each gas constituent and also indicated that insignificant changes in amounts occurred during the transportation period. As shown in Table 11, the atmosphere had very little water vapor; this, from a microbial lethality standpoint, was desired.

The 2% oxygen concentration level for the canister atmosphere during the cycle was determined after the data from the dummy run was available and indicated that this level (or less) could be maintained during the sterilization test. The oxygen concentration profile that was actually achieved during the feasibility model sterilization is shown in Fig. 21. The oxygen concentration was

Table 11. Capsule atmosphere, feasibility model sterilization change during transportation

Constituent	After backfilling 25-ft simulator, mole %	Before purging terminal sterilization chamber,[a] mole %
Oxygen	0.19	0.61
Nitrogen	99.8	99.3
Argon	0.03	0.05
Water vapor	<0.008	<0.006

[a]Measurement taken 1.5 h after backfilling.

below 2% in the canister at all times when the temperature of the canister was above 80°C. Thus, the intent of the test requirement was satisfied. Although the *Voyager* requirement* of ¼% oxygen could be achieved during evacuation and backfilling, the ¼% would be difficult to maintain in any portable facility (such as the terminal sterilization chamber); therefore, it was not a test requirement for CSAD. It should be emphasized, however, there is an unanswered question concerning the oxygen concentration that can be tolerated at high temperature without seriously degrading materials and components.

The temperature responses were as predicted as is shown in Fig. 22. This comparison shows that the first thermal model more closely represented the actual thermal responses than the conservative model. The measurement that controlled the determination of the sterilization cycle was the lander center node, the thermocouple

*"Environmental Specification, *Voyager* Flight Capsule Equipment, Type Approval and Flight Acceptance Test Procedure for the Heat Sterilization and Ethylene Oxide Decontamination Environments," VOL-50503-ETS. Jet Propulsion Laboratory, Pasadena, Calif., Jan. 12, 1966 (available to authorized personnel).

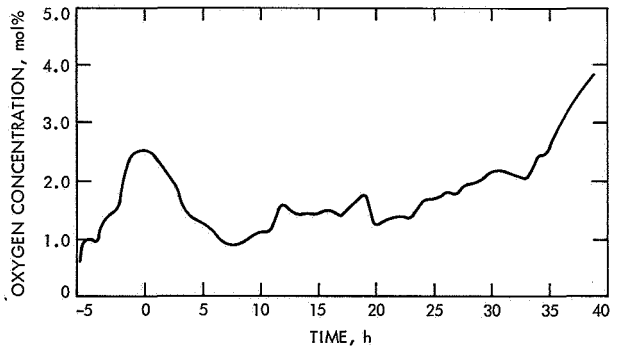

Fig. 21. Oxygen concentration profile, CSAD feasibility model sterilization

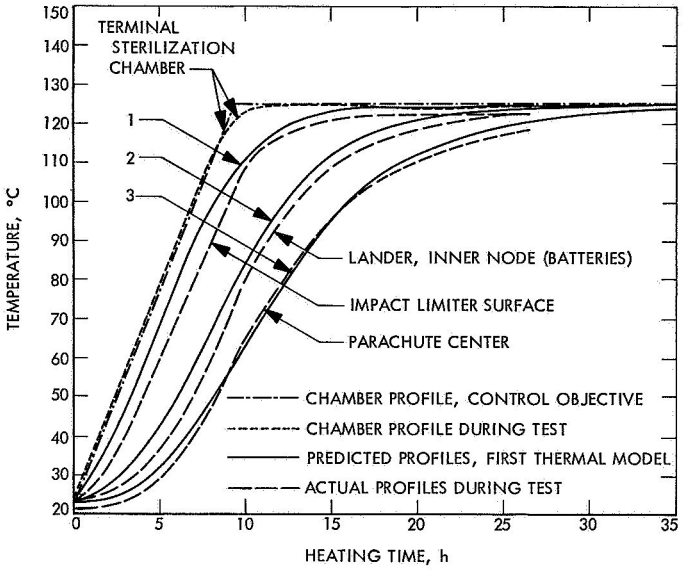

Fig. 22. Actual vs predicted heating profiles, CSAD feasibility model sterilization

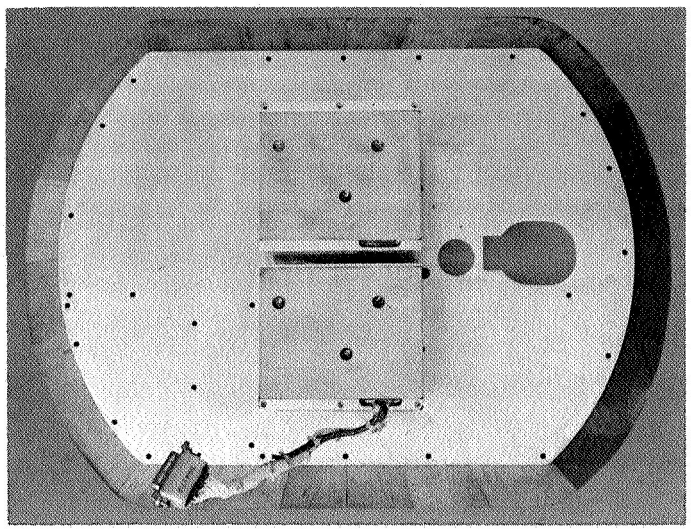

Fig. 23. Batteries attached to underside of lander cover

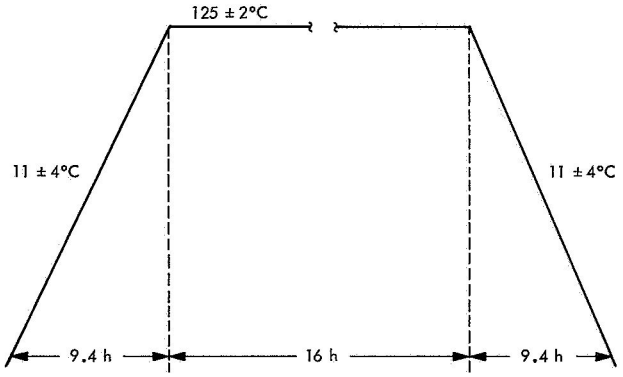

Fig. 24. Terminal sterilization chamber temperature profile, CSAD feasibility model sterilization

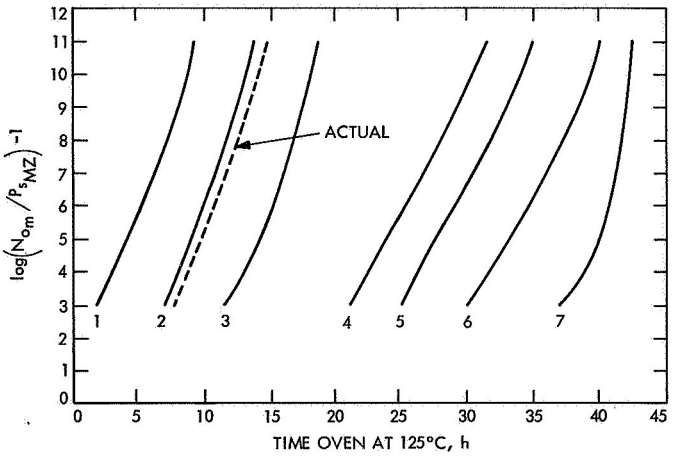

Fig. 25. CSAD terminal sterilization chamber time at temperature with actual parametric curve

in the battery. Although the battery location was an interior one (Fig. 23), it was demonstrated during the separate sterilization test of the lander that the lander chassis and modules behave nearly isothermally with the battery lagging the others by 1°C. Therefore, to be conservative, the battery measurement was chosen, after initiation of the test, as being representative of the mated surface location with the greatest thermal lag. Since the actual profile is between the predicted profiles 2 and 3, the parametric curve 3 in Fig. 15 (which is based on profile 3) was the one used to determine the terminal sterilization chamber time at temperature.

The necessary microbial reduction was based on the microbial estimates from the bioassay (Table 9). The number of spores on the mated surfaces of the lander was estimated to be 1635. It was assumed that all of these spores were at the mated surface location with the greatest thermal lag. The probability of survival on the mated surfaces of the lander was 10^{-4}. Therefore, the value of $\log (N_{o_m}/P_{s_{MZ}}) - 1$ was 6.223. The chamber time at temperature of 15.5 h was then read from Fig. 15. The next hour (16) was the time chosen for the actual sterilization process used for the CSAD feasibility model as shown in Fig. 24.

Based on the battery temperature profile, *a posteriori* process calculations have been performed. The resultant terminal sterilization chamber time at temperature is shown as the dashed curve in Fig. 25. By extrapolating

the curve to 16 h of exposure at 125°C, a decade reduction of 14 could have been accommodated during the sterilization cycle. This means that an initial burden of 10^{11} could have been present on the most heat resistant mated surfaces of the lander, and the process still would have achieved the appropriate level of survival probability. Or, equivalently, the probability of survival of one or more organisms from the initial burden present would be slightly greater than 10^{-12}. Consequently, the CSAD feasibility model sterilization process was representative of a conservative process that might be used to terminally sterilize a flight capsule.

VII. Conclusions

The most significant benefit of the CSAD sterilization program was the experience with the procedures, operations, and facilities necessary to satisfy the planetary quarantine requirements. The CSAD project served as a pilot operation for a project that would have to meet planetary quarantine requirements. Burden estimating methods were established and maintained, capsule thermal models were developed, and a terminal heat sterilization cycle was designed and carried out. It is believed that the procedures developed and used on the feasibility model would satisfy the NASA quarantine requirements in the area of applicability.

VIII. Recommendations for Future Programs

As the CSAD program progressed, areas requiring additional study or investigation were noted. Also, in reviewing the sterilization program at the conclusion of the project, recommendations on approaches for future programs could be listed.

A. Areas Requiring Further Investigation

The following areas are recommended for investigation during future programs.

(1) Assembly level flight acceptance sterilization tests. The method for establishing these requirements should be carefully examined. If a future sterilization program is based on the CSAD approach, it will be necessary to verify either experimentally or analytically that the assembly level sterilization cycle will yield sterilized interiors for all types of space hardware.

(2) Monitoring data. The significance of the monitoring data, as well as approaches for interpreting the results, require additional study so that future programs can achieve acceptable results with a minimum expenditure of time and funds.

(3) Oxygen concentration during sterilization. The level of oxygen concentration that can be tolerated by space hardware when subjected to high temperatures requires further definition.

(4) Post-sterilization activities. These activities were not considered in this study, but would require emphasis for flight programs.

B. Approaches for Future Programs

A coordinated effort should be initiated early in a project for the purpose of optimizing the thermal design of the capsule and minimizing the severity and complexity of the terminal sterilization process. If the engineers responsible for the design of thermal control systems are unfamiliar or unaware of the methods of implementing the sterilization requirements and design the vehicle solely for spaceflight, serious problems could arise during the performance of the sterilization cycle that may compromise the planetary quarantine constraints or that may degrade the capsule equipment.

The analytical concepts for establishing process parameters as outlined in Section IV and detailed in Ref. 1 could be applied to any future program. Computer programs to perform these calculations have been written and are readily available from the Computer Software Management Information Center at the University of Georgia. The title of the programs are SPAN and SPAN-C, which stand for Sterilization Process Analysis Network. (SPAN uses temperature profiles input by tape; SPAN-C uses temperature profiles input by cards.) The programs are very versatile. For example, they may be used not only for terminal sterilization computations but also to calculate a measure of the lethality that occurs on a capsule subsystem adjacent to an internal heat source, such as an RTG (radioisotope thermoelectric generator).

To demonstrate that a capsule has met the sterilization requirements, it should be shown that:

(1) Interiors have been sterilized either during flight acceptance testing or at some point in the assembly and test sequence.

(2) The process parameters of the terminal sterilization cycle have been properly imposed on the capsule and laboratory experiments show that the imposi-

tion of process parameters produce the required probability of sterility.

The thermal analytical model of the capsule should be continually updated as additional information for sterilization tests on nonflight capsules (such as thermal control model or proof test model) becomes available. Since it is desirable to limit the number of capsule temperature measurements during the sterilization cycle, good prediction of thermal behavior is required. (Flight transducers can be used, but this provision for monitoring during sterilization must be incorporated into the capsule design.)

References

1. Hoffman, A. R., and Stern, J. A., *Terminal Sterilization Process Calculation for Spacecraft*, Technical Report 32-1209. Jet Propulsion Laboratory, Pasadena, Calif., Nov. 15, 1967. (Also appears in *Develop. Ind. Microbiol.*, Vol. IX, pp. 49–64, 1968.)
2. Craven, C. W., Stern, J. A., and Ervin, G. F., "Planetary Quarantine and Space Vehicle Sterilization," *Astronaut. Aeronaut.*, pp. 19–48, Aug. 1968.
3. Stumbo, C. R., *Thermobacteriology in Food Processing*. Academic Press, New York and London, 1965.
4. *NASA Standard Procedures for the Microbiological Examination of Space Hardware*, NHB 5340.1. National Aeronautics and Space Administration, Washington, D. C., Aug. 1, 1967.
5. Angelloti, R., and Litsky, W., "Comparative Evaluation of the Cotton Swab and Rodac Methods for the Recovery of Bacillus Subtilis Spore Contamination from Stainless Steel Surfaces," *Health Lab Sci.*, Vol. I, pp. 289–296, Oct. 1964.

Appendix

Comparisons of Predicted Temperature Profiles vs Test Data for CSAD Feasibility Model Sterilization

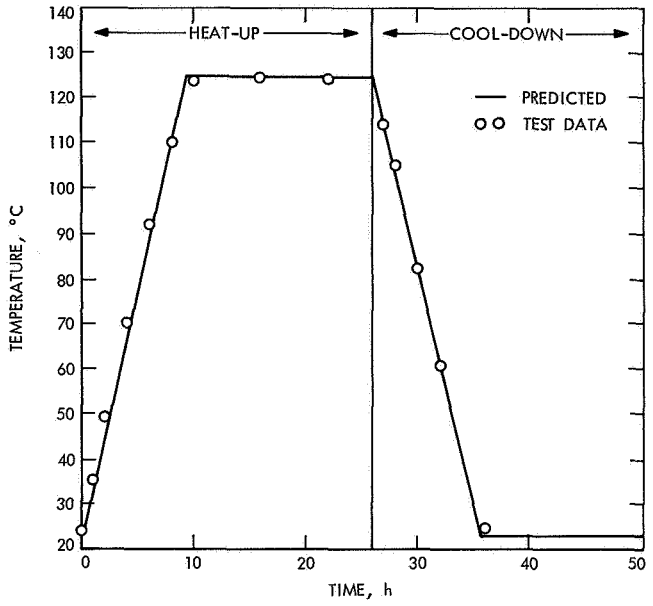

Fig. A-1. Terminal sterilization chamber

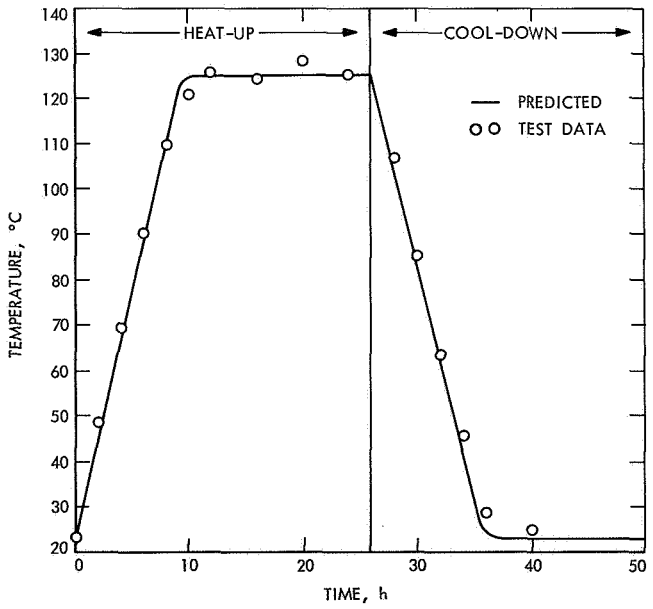

Fig. A-2. Sterilization canister, fore

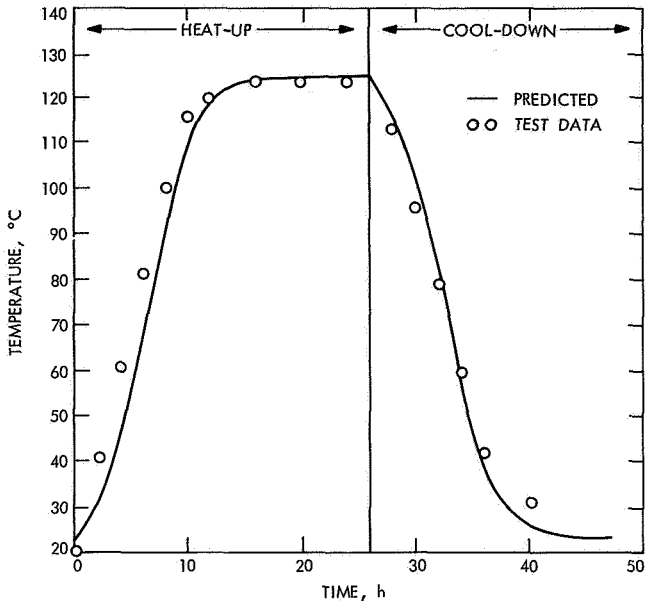

Fig. A-3. Aeroshell exterior surface

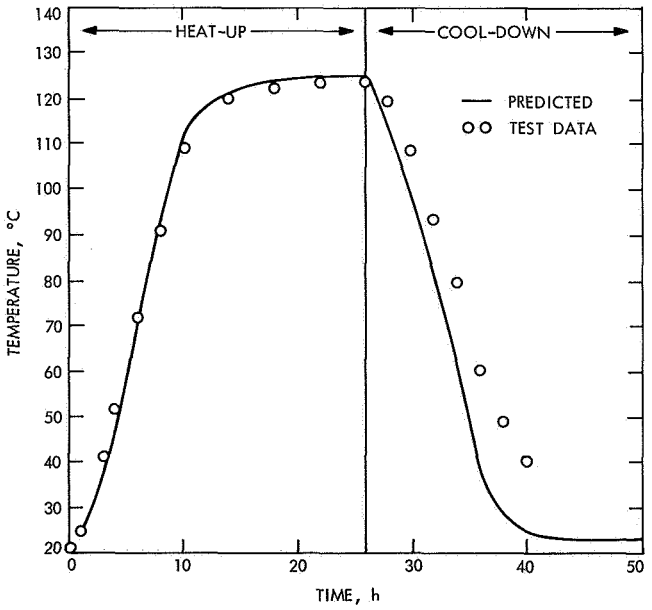

Fig. A-4. Aeroshell interior surface

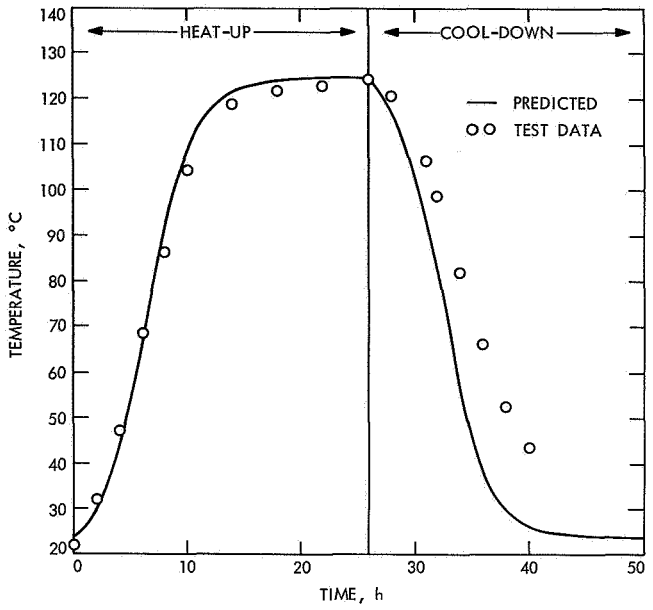

Fig. A-5. Mass spectrometer

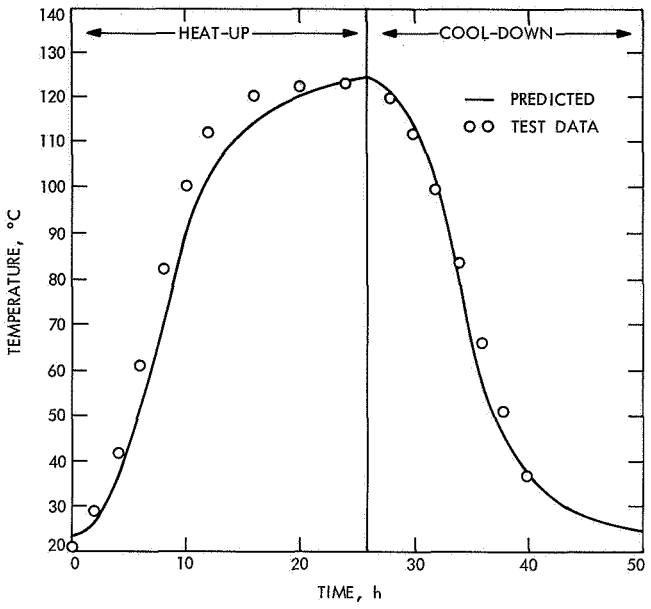

Fig. A-7. Entry electronics battery chassis

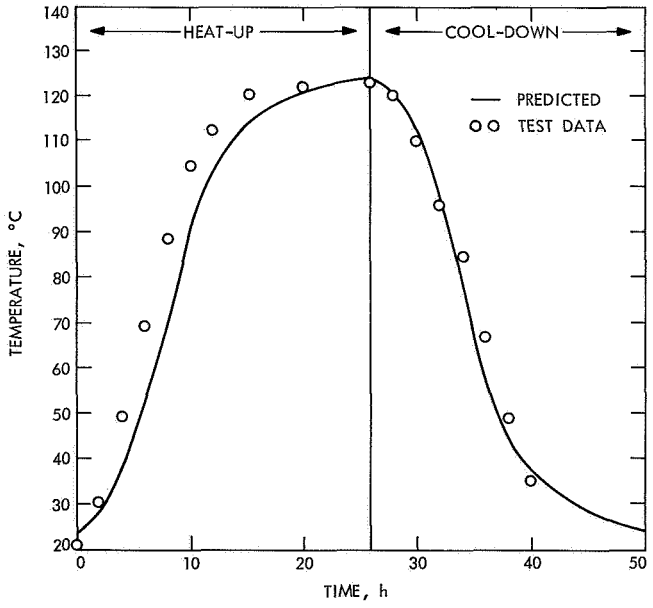

Fig. A-6. Entry electronics radio module

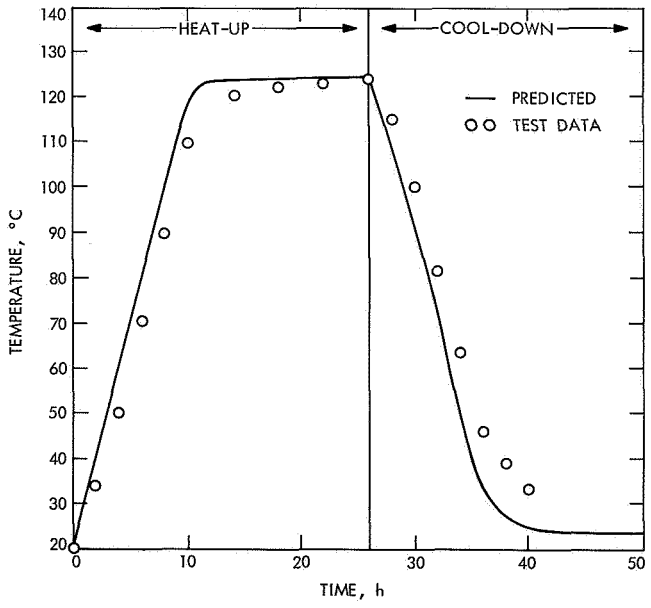

Fig. A-8. Impact limiter surface

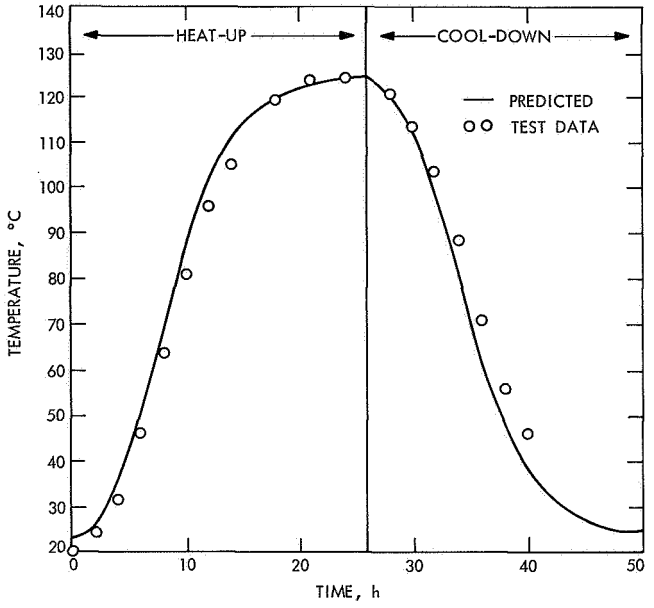

Fig. A-9. Lander, cover on parachute side

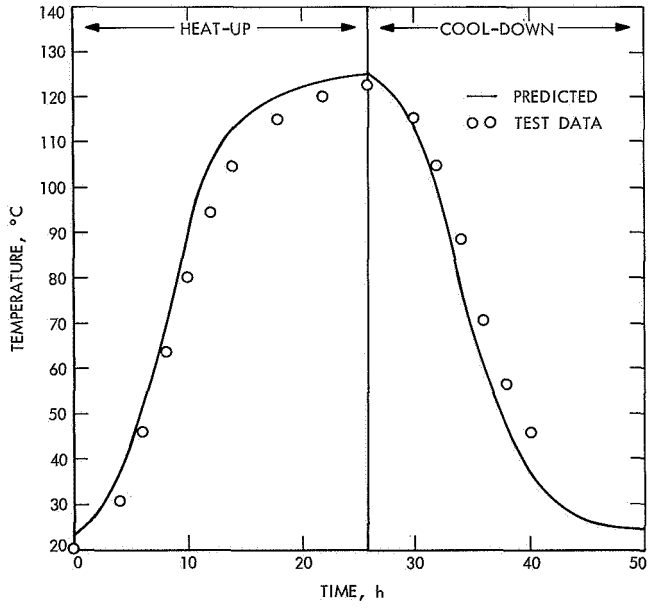

Fig. A-10. Lander, battery center

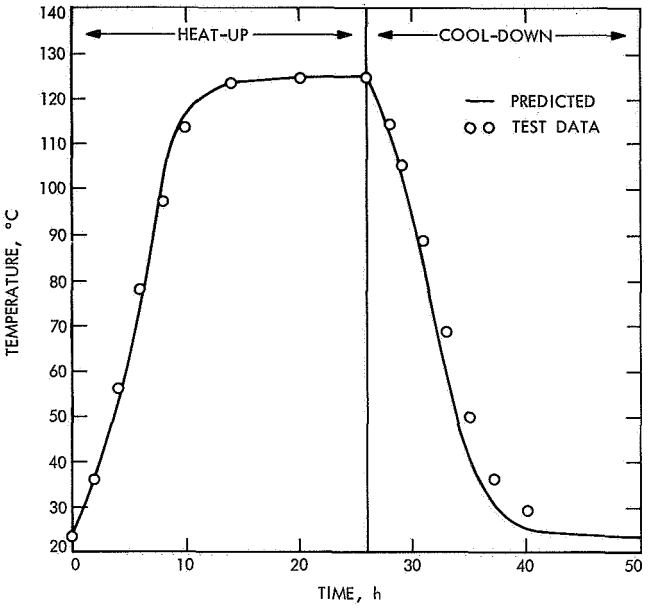

Fig. A-11. Relay antenna surface

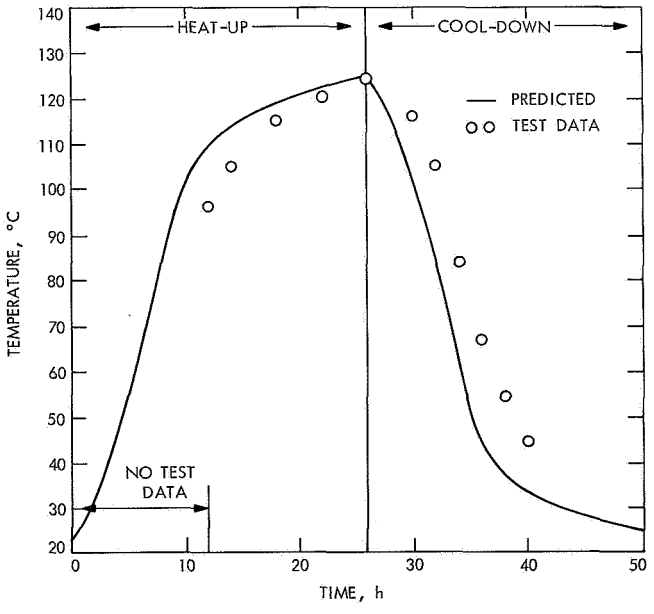

Fig. A-12. Parachute canister surface

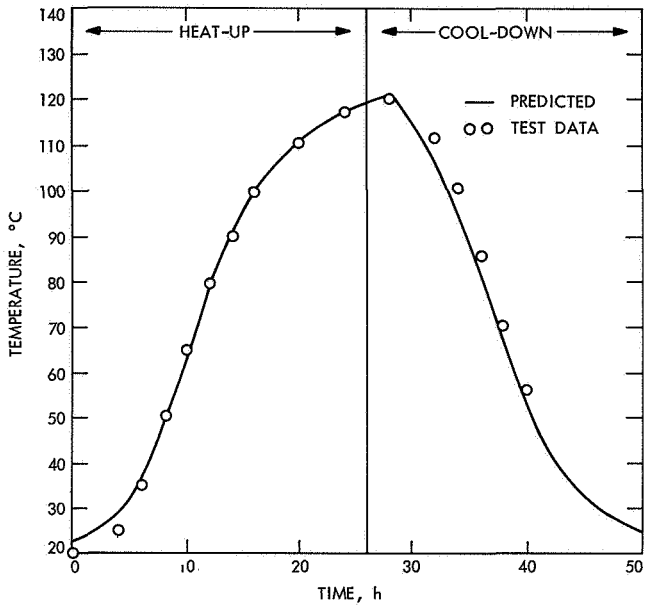

Fig. A-13. Parachute center